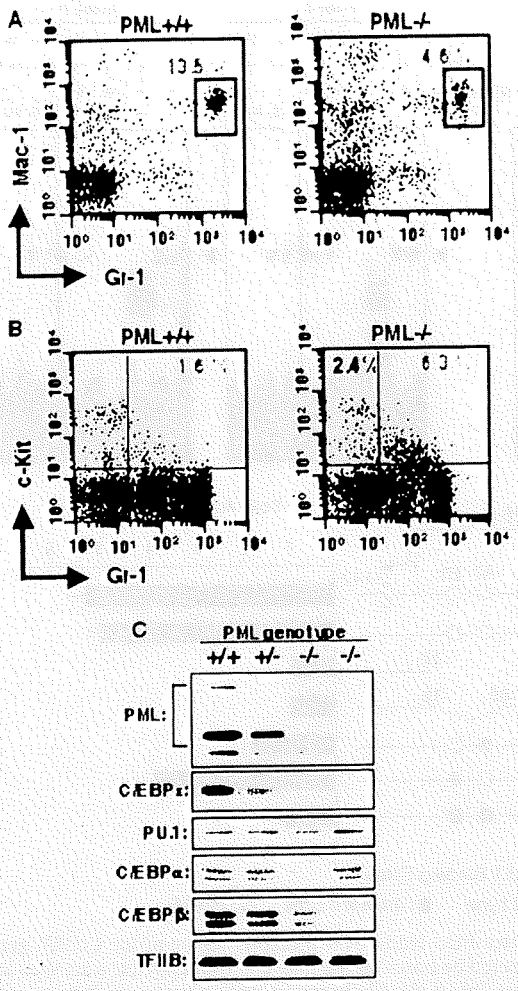

FIG. 1. Impaired granulopoiesis in *PML*$^{-/-}$ mice. (A) Mature granulocytes were reduced in peripheral blood of *PML*$^{-/-}$ mice. Whole peripheral blood cells were stained with anti-Mac-1 and anti-Gr-1 and then analyzed by flow cytometry. (B) Immature granulocytes were increased in BM of *PML*$^{-/-}$ mice. BM cells were stained with anti-Gr-1 and -c-Kit. (C) Reduced expression of C/EBPε in BM mononuclear cells from *PML*$^{-/-}$ mice. Total cell lysates were analyzed by Western blotting.

There was no significant difference in PU.1 and C/EBPα, but C/EBPβ expression was modestly reduced in *PML*$^{-/-}$ mice. On the other hand, C/EBPε expression was reduced in proportion to that of PML (Fig. 1C). These results suggest that the specific involvement of PML in C/EBPε expression may account for its underlying role in granulocytic differentiation.

***C/EBPε* is a direct transcriptional target of PU.1.** To investigate how PML is involved in C/EBPε expression, we first analyzed its promoter. The transcription of the *C/EBPε* gene is regulated mainly by the downstream Pβ promoter, which is highly conserved among different species (2, 34). The DNA sequence around the Pβ promoter is highly rich in purine tracts, which are peculiar features of myeloid cell-specific genes and often serve as potential binding sites for *ets* family transcription factors. These facts prompted us to examine if PU.1 regulates the expression of *C/EBPε*. ChIP assays of HL-60 cells revealed that PU.1 binds to the region 2, which includes the Pβ promoter, in vivo (Fig. 2A). However, we could not detect any significant binding of PU.1 to other genomic regions 4 kb upstream or downstream of the Pβ promoter (regions 1 and 3, respectively). These results indicate that PU.1 binds to a specific genomic region that includes the Pβ promoter. The specificity of this ChIP assay was further confirmed, as the same anti-PU.1 antibody failed to precipitate region 2 in MOLT-4 cells that lack endogenous PU.1 expression (see Fig. S1A in the supplemental material). EMSA detected at least two PU.1 binding regions: region A, between bp −80 and −44, and region B, between bp −40 and −18. PU.1 bound to region A more efficiently than region B (Fig. 2D, left). Inspection of the DNA sequence identified six putative *ets* core motifs (A1 to A3 and B1 to B3) (Fig. 2C). To identify the PU.1 binding sites, we constructed a *C/EBPε* promoter-containing luciferase reporter, introduced either several block mutations or various combinations of site-directed mutations into these motifs, and performed transactivation assays using NIH 3T3 cells (Fig. 2E). As we expected, the response to PU.1 was limited to a region between bp −80 and −18, which contains a purine-rich tract. Luciferase assays further revealed that the response to PU.1 was mediated between positions bp −62 and −57 (A2) and between bp −34 and −29 (B1) (Fig. 2E). Similar results were also obtained for HeLa cells (see Fig. S1B in the supplemental material), suggesting that these effects do not depend on the cell context. Competitive EMSA combined with supershift assays indicated that PU.1 specifically binds to these sites in vitro (Fig. 2D, middle and right panels). Taken together, these results show that PU.1 transactivates the *C/EBPε* gene directly.

PML IV associates with PU.1 in vivo. To investigate the interaction of endogenous PML and PU.1, an immunoprecipitation assay was performed using HL-60 cells. An anti-PML antibody raised against its N terminus successfully immunoprecipitated multiple PML isoforms (Fig. 3A) from HL-60 cell extracts and also pulled down PU.1 together with them (Fig. 3B, left). Reciprocal experiments using an anti-PU.1 antibody revealed the predominant coimmunoprecipitation of a specific PML isoform with a molecular mass of ~75 kDa (Fig. 3B, right). These results indicate the association of these endogenous proteins in myeloid lineage cells. To determine the isoform specificity for PU.1 binding, PU.1 and one of each of the PML isoforms were transiently coexpressed and subjected to immunoprecipitation. PML II and IV specifically interacted with PU.1 (Fig. 3C). An association between PU.1 and the other isoforms, including PML VI, was not successfully detected.

To further confirm those results, we next examined whether these two proteins are colocalized in cells (Fig. 3D). Immunofluorescence revealed that PU.1 was spread throughout the nucleus in NIH 3T3 cells. Upon cotransfection with PML IV, however, PU.1 formed discrete speckles and colocalized prominently with PML IV PODs. Surprisingly, and in contrast with the immunoprecipitation results, PU.1 was not recruited to PML II PODs but instead was recruited to PML VI PODs. Colocalization of PU.1 with both PML IV and VI was also observed in HeLa cells (data not shown). We further examined the subcellular localization of both proteins in mouse embryonic fibroblasts from *PML*$^{-/-}$ mice. Here, we found that PU.1 was also recruited to PML IV PODs but not to PML VI PODs

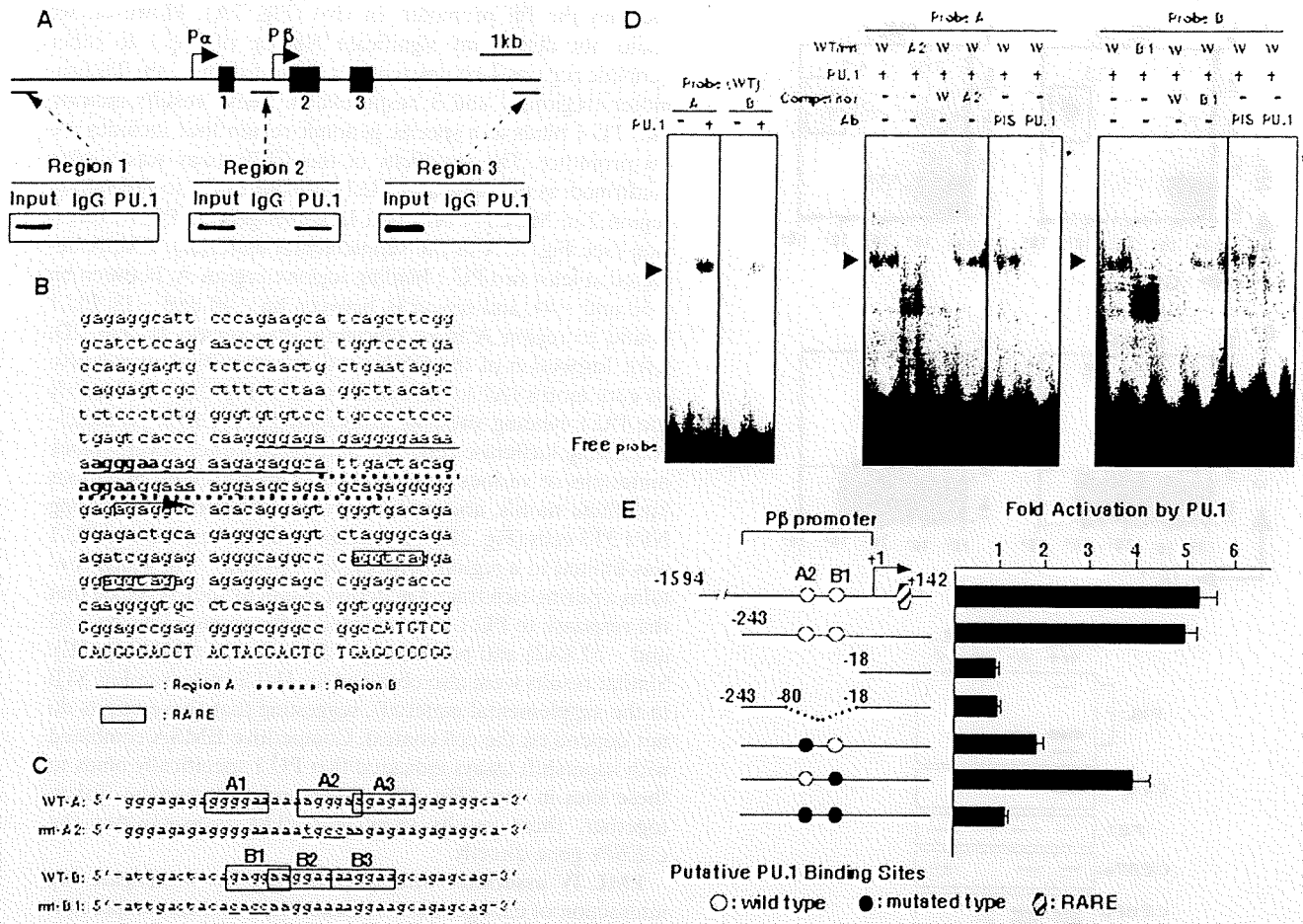

FIG. 2. PU.1 regulates the expression of the *C/EBPε* gene. (A) A ChIP assay shows that PU.1 binds to the promoter region of the *C/EBPε* gene in HL-60 hematopoietic cells. In the schematic of the *C/EBPε* locus, exons are represented by boxes on the line, and transcription start sites are represented by arrows. Three regions examined for PU.1 binding are indicated. Cross-linked HL-60 chromatin was immunoprecipitated with anti-PU.1 antibody (PU.1) or isotype-matched immunoglobulin G (IgG) as a negative control. Three percent of input DNA was also PCR amplified. (B) DNA sequences of the *C/EBPε* promoter region. A major transcriptional start site is indicated by an arrow. The oligonucleotide sequences used for EMSA probes are underlined, and the putative PU.1 binding sites are shown in boldface type. The RARE is shown in boxes. (C) Sequences of wild-type (WT) and mutated (mt) probes used for EMSA. The six putative core PU.1 binding motifs are shown in boxes, and the two PU.1 binding sites tested by EMSA are shown in boldface type. The mutated nucleotides are underlined. (D) Identification of PU.1 in DNA-protein complexes by EMSA using nuclear extracts from BOSC23 cells transfected with the PU.1 expression vector. Arrowheads indicate the PU.1-DNA complexes. Supershifted bands are indicated by asterisks. PIS, rabbit preimmune serum. (E) PU.1 response elements within the *C/EBPε* promoter were confirmed by luciferase reporter assays. A major transcriptional start site is shown as "+1." NIH 3T3 cells were transfected with 0.1 μg of wild-type reporter plasmids containing the region between bp −1594 and +142 or bp −243 and +142 or its mutant derivatives along with 0.1 μg of a PU.1 expression vector. The results are represented as activity (*n*-fold) compared to that of PU.1 and are the average of at least three independent experiments. The error bars represent the standard deviations.

(see Fig. S2 in the supplemental material). These results suggest that the in vivo association between PU.1 and PML IV is of primary importance and that PML VI might indirectly associate with PU.1, although underlying mechanisms remain to be elucidated.

PML IV specifically cooperates with PU.1 to induce terminal differentiation of L-G myeloblasts. We next investigated the ability of each PML isoform to cooperate with PU.1 in the terminal differentiation of L-G myeloid progenitor cells (16). L-G cells were transfected with a vector for expressing PU.1 under the control of a metallothionein promoter (pMT-PU.1). We established several stable clones and confirmed that they morphologically differentiated toward polymorphonuclear cells (PMNs) upon the induction of PU.1 with $ZnSO_4$. To investigate the isoform-specific cooperation between PU.1 and PML, we used a retrovirus to transduce the L-G/MT-PU.1 cells with PML I, II, III, IV, V, VI, or mock (L-G/MT-PU.1/PML isoforms) (Fig. 4A). The level of PU.1 expression following induction with $ZnSO_4$ was the same in all seven cotransfected cells and the parent L-G/MT-PU.1 cells (see Fig. S3A in the supplemental material) (data not shown). Although the expression level of transduced PML IV seemed to be high compared to that of the endogenous one, it was almost comparable to the level of total PML expression (see Fig. S3C in the supplemental material). The induction of PU.1 expression alone retarded cell growth, and the coexpression of PML IV enhanced this effect (Fig. 4B). PU.1 and PML IV also had a synergistic effect on morphological differentiation (Fig. 4C).

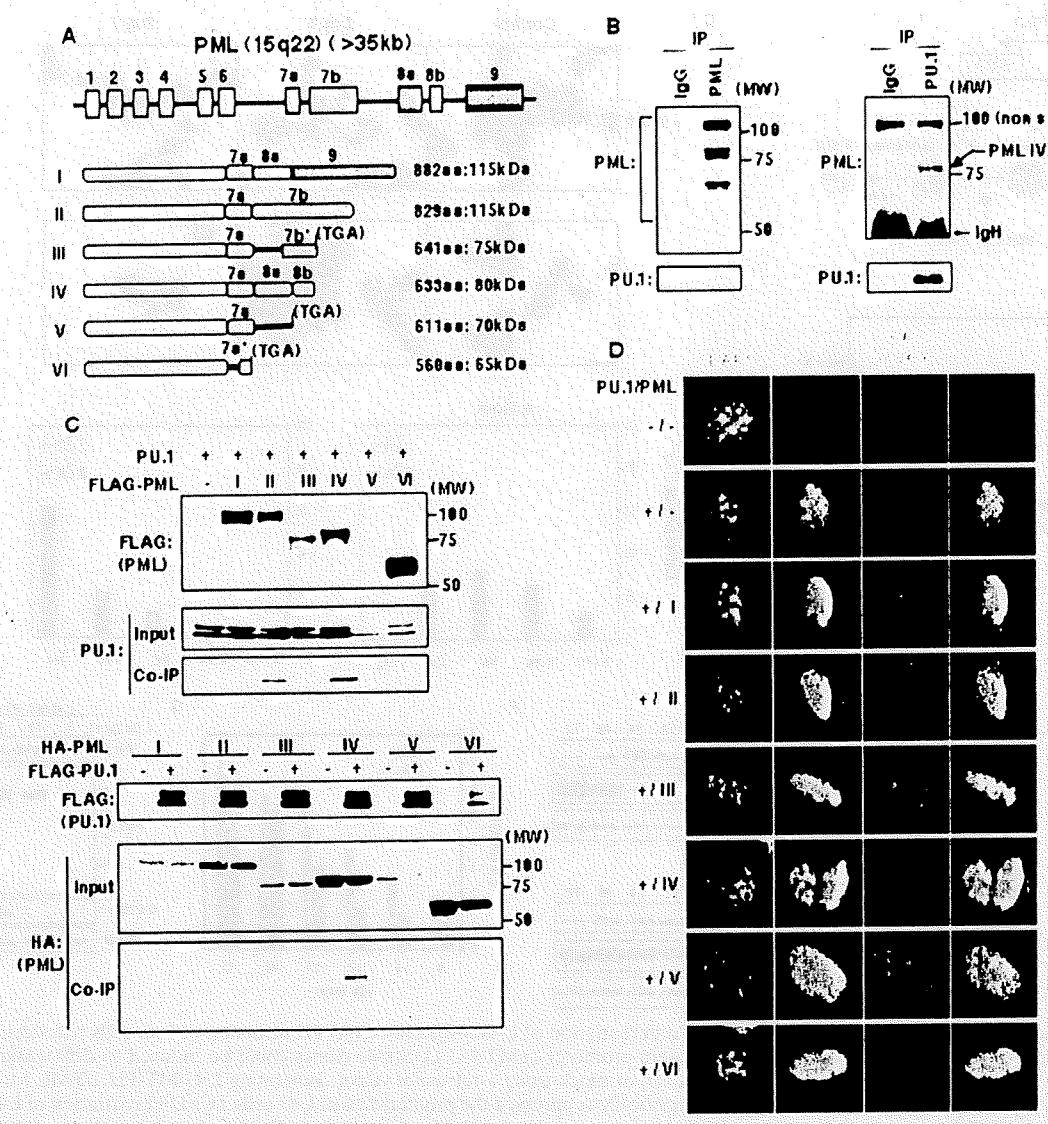

FIG. 3. PML associates with PU.1 in vivo. (A) Schematic illustration of the genomic structure of the *PML* gene. Boxes represent exons, and their exon numbers are indicated. Six major alternatively spliced isoforms are shown. The solid lines indicate retained introns. Asterisks show frameshifts of the coding sequence compared to PML II. Numbers of amino acid (aa) residues and the apparent molecular masses of each isoform are given. (B) Association of endogenous PU.1 and PML. Total cell lysates from HL-60 cells were immunoprecipitated with an anti-PML (left) or an anti-PU.1 (right) antibody and then analyzed by Western blotting. Note that PML, with a molecular mass of ~75 kDa, was coprecipitated predominantly with PU.1. IgG, immunoglobulin G. (C) PU.1 coimmunoprecipitates with PML II and IV. Total cell lysates from BOSC23 cells transfected with the indicated expression vectors were subjected to immunoprecipitation with an anti-FLAG antibody and then analyzed by Western blotting. The antibodies used for Western blotting are indicated on the left of each panel. IP, immunoprecipitates; MW, molecular weight (in thousands). (D) PU.1 and PML IV were colocalized within PODs. The expression vectors indicated were transiently coexpressed in NIH 3T3 cells and then costained with antibodies to PU.1 and HA (for PML). DAPI, 4′,6′-diamidino-2-phenylindole.

After 7 days of culture with $ZnSO_4$, most of the control mock-transfected cells (L-G/MT-PU.1/mock) differentiated around the metamyelocyte stage, and only a few mature PMNs were observed. In contrast, more than 60% of L-G/MT-PU.1/PML IV cells differentiated into mature PMNs. The PML VI isoform cooperated moderately with PU.1 to induce granulocytic differentiation (see Fig. S3D in the supplemental material). The other PML isoforms (I, II, III, and V), however, did not affect PU.1-induced differentiation of L-G cells (data not shown). It is noteworthy that the cooperativity of PU.1 and PML isoforms in granulocytic differentiation was comparable to their POD colocalization capability.

Next, we examined the effect of PML IV on PU.1 transcription activity. Luciferase reporter assays showed that among six PML isoforms, only PML IV had a marked effect on the activation of the *C/EBPε* reporter by PU.1 (Fig. 4D). A parallel experiment using a reporter of the *M-CSFR* promoter also demonstrated a specific cooperation between PU.1 and PML IV, indicating that the interaction between these two proteins does not depend on the promoter context (see Fig. S3E in the supplemental material).

Moreover, we next examined whether PML IV could affect the expression of endogenous C/EBPε during PU.1-induced granulocytic differentiation (Fig. 4E). In L-G/MT-PU.1/mock

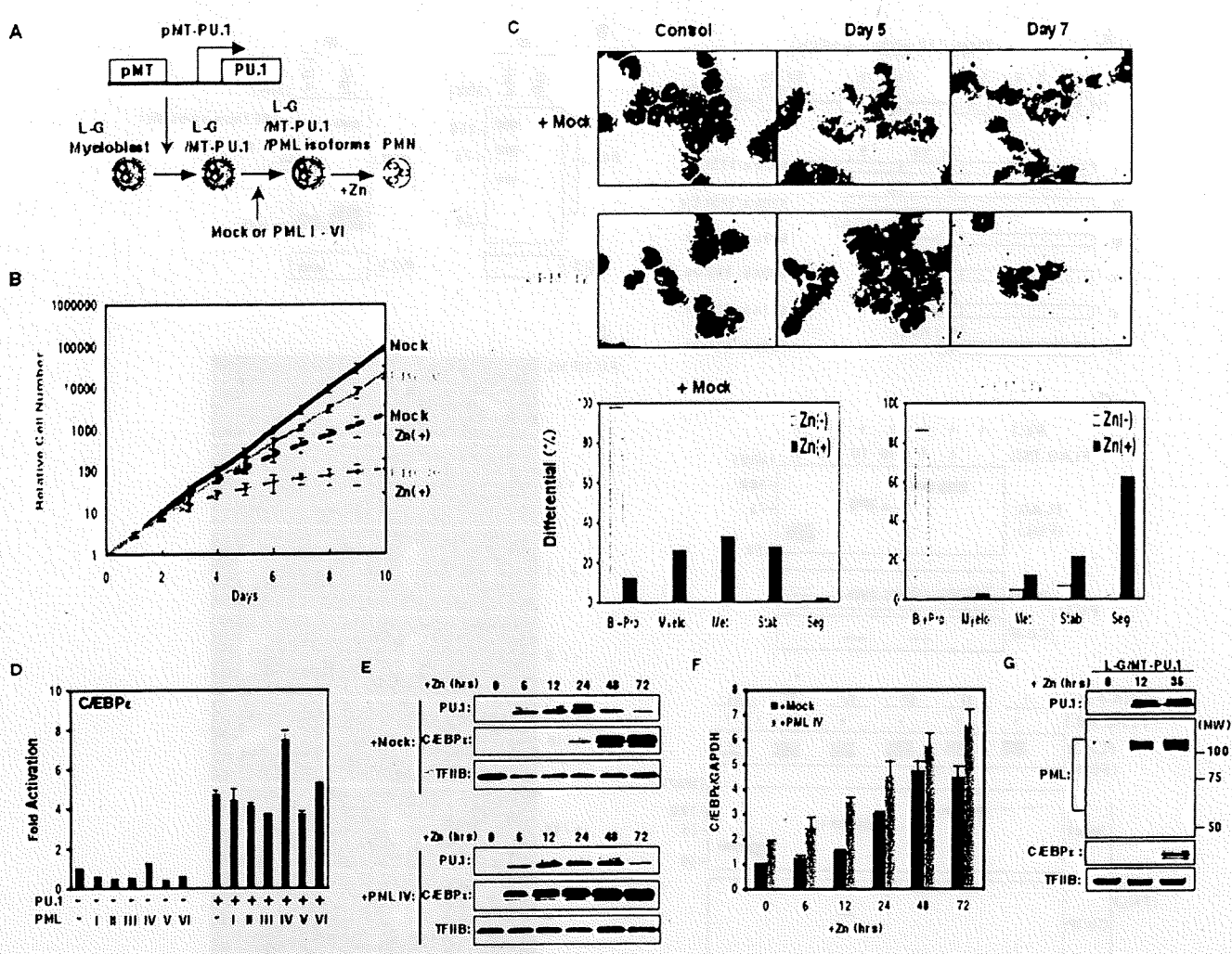

FIG. 4. PML IV and PU.1 cooperate to accelerate terminal differentiation of L-G myeloblasts. (A) Construction of L-G cells transfected with a plasmid encoding PU.1 under the control of the metallothionein promoter (pMT-PU.1). Stable clones could be induced to differentiate into PMNs. The cells were further transformed with each PML isoform or mock using a retroviral vector, generating L-G/MT-PU.1/PML I to VI or mock, respectively. (B) Upon expression of PU.1, PML IV synergistically suppressed the proliferation of L-G cells. (C) Differentiation of L-G cells upon induction of PU.1 by $ZnSO_4$ treatment. Cytospin-prepared cells were stained with May-Giemsa stain (top) and evaluated by morphological criteria after 7 days (bottom). Bl, blast; Pro, promyelocyte; My, myelocyte; Met, metamyelocyte; Stab, stab cell; Seg, PMNs. (D) PML IV specifically enhances PU.1-induced activation of the *C/EBPε* promoter-containing luciferase reporter in NIH 3T3 cells. The effector plasmids are indicated. (E) Western blotting shows that PML IV and PU.1 synergistically enhance the expression of C/EBPε in L-G cells. (F) Real-time RT-PCR was used to quantify *C/EBPε* mRNA in L-G/MT-PU.1/mock and PML IV cells treated with $ZnSO_4$ for the indicated times. All results are given in relative units compared to *GAPDH*. Result are means ± standard deviations of triplicate determinations of a representative experiment. Note that PCR detects all *C/EBPε* mRNA isoforms generated by the alternative use of promoters or splicing. (G) Western blotting shows that the expression of endogenous PML protein increases during PU.1-induced granulocytic differentiation. MW, molecular weight (in thousands).

cells, C/EBPε expression started to increase 24 h after exposure to $ZnSO_4$, and it reached a maximum after 48 to 72 h. On the other hand, the coexpression of PML IV enhanced C/EBPε expression within 6 h after $ZnSO_4$ treatment in parallel with PU.1 expression. The PML VI isoform modestly promoted PU.1-induced C/EBPε expression. The other PML isoforms (I, II, III, and V), however, did not affect PU.1-induced expression of C/EBPε (see Fig. S3F in the supplemental material).

To confirm that PML IV enhancement of C/EBPε expression was due to transcriptional activation, quantitative RT-PCR was performed (Fig. 4F). In L-G/MT-PU.1/PML IV cells, all six time points showed elevated *C/EBPε* transcripts compared to L-G/MT-PU.1/mock cells. The difference was more prominent before C/EBPε expression started to increase in L-G/MT-PU.1/mock cells.

We next investigated why more than 12 h was required before the induction of C/EBPε expression in LG/MT-PU.1 cells in spite of possible direct regulation by PU.1. Western blots showed that PU.1 induced the expression of endogenous PML in L-G/MT-PU.1 cells (Fig. 4G). PML expression did not increase after $ZnSO_4$ treatment in either parent L-G cells or L-G/MT-PU.1 cells driven to differentiate into granulocytes by treatment with granulocyte colony-stimulating factor instead of interleukin-3 (see Fig. S3G in the supplemental material). These results indicate that endogenous PML expression is specifically regulated by PU.1. Since quantitative

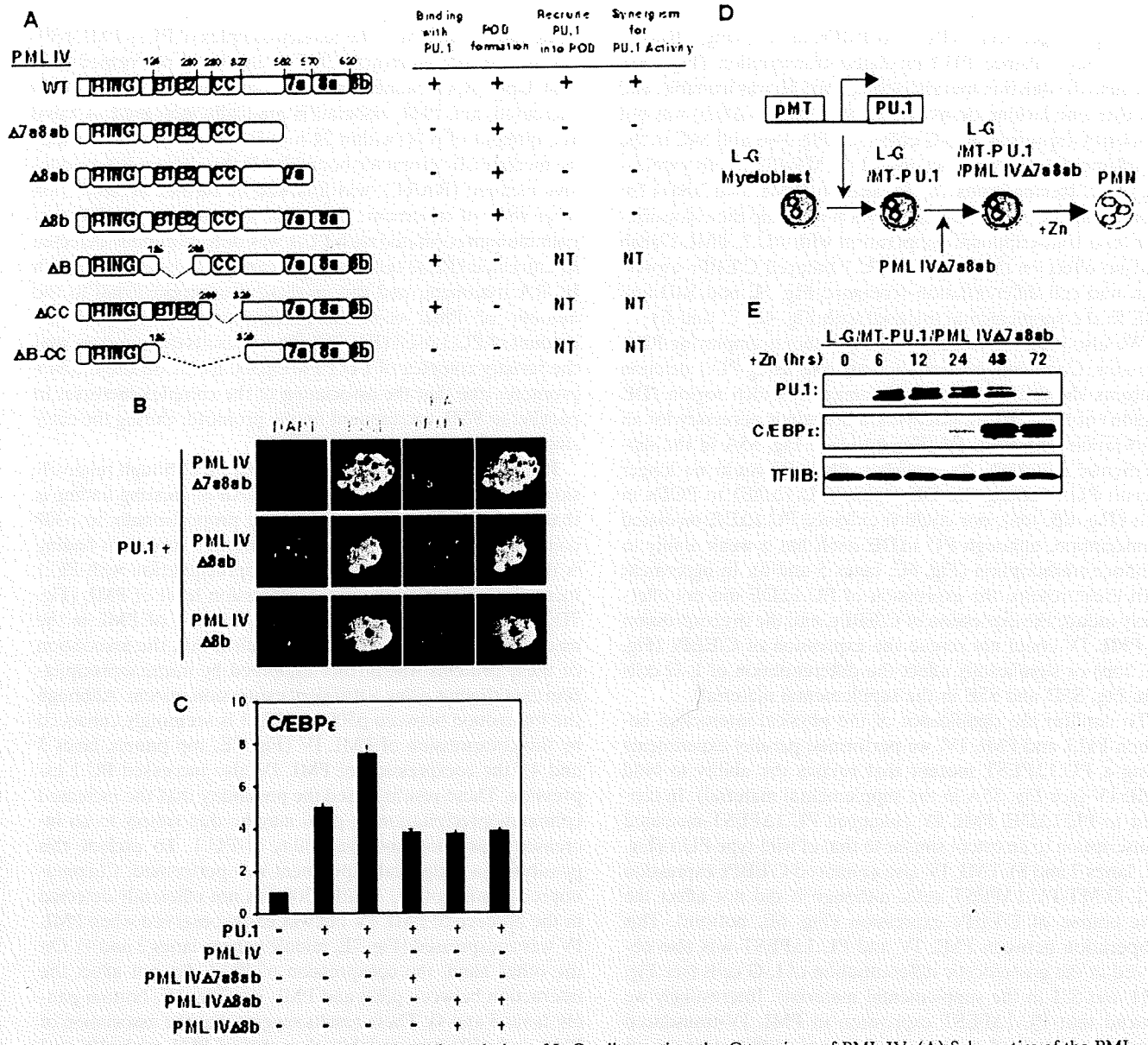

FIG. 5. Enhancement of PU.1-induced terminal differentiation of L-G cells requires the C terminus of PML IV. (A) Schematics of the PML IV mutants and summary of the domain mapping of the physical and functional interaction with PU.1. Pro, proline-rich region; RING, RING finger domain; B1 and B2, B boxes; CC, coiled-coil domain; WT, wild type; NT, not tested. (B) Immunofluorescence shows that the PML IV C-terminal deletion mutants do not colocalize with PU.1 in NIH 3T3 cells. DAPI, 4′,6′-diamidino-2-phenylindole. (C) Luciferase reporter assays show that PML IV C-terminal deletion mutants do not enhance PU.1-induced transcription in NIH 3T3 cells. (D) Schematics of the construction of PU.1-inducible L-G cells transduced with a PML IV C-terminal deletion mutant (L-G/MT-PU.1/PML IVΔ7a8ab) or mock (L-G/MT-PU.1/mock). (E) Western blots show that the PML IVΔ7a8ab is unable to enhance PU.1-induced expression of C/EBPε in L-G cells.

RT-PCR analysis revealed that endogenous *PML* mRNA also increased (data not shown), PU.1 regulates PML expression, at least in part, at the transcriptional level. An important finding is that C/EBPε expression was also induced in a fashion parallel to that of PML expression in L-G/MT-PU.1 cells (Fig. 4G). Together with the finding that the induction of C/EBPε becomes much faster when PML IV is already expressed exogenously (see Fig. S3H in the supplemental material), these results clearly indicate that PU.1 action on *C/EBPε* transcription is modulated by PML.

Structure-function relationship of the PU.1-PML IV interaction and its relevance in myeloid terminal differentiation. We performed coimmunoprecipitation assays to determine the region of PML required for the association with PU.1. Deletion of the C-terminal 13 amino acids of PML IV, which corresponds to the isoform-specific exon 8b, completely abolished the formation of the PU.1-PML complex (Fig. 5A) (see Fig. S4A in the supplemental material). The integrity of B boxes and the coiled-coil region was also required for an association with PU.1 (Fig. 5A) (see Fig. S4A in the supplemental mate-

rial). In addition, these C-terminally-deleted PML mutants could no longer recruit PU.1 to PODs in vivo (Fig. 5B), nor could they enhance PU.1-mediated transcription (Fig. 5C). Because the deletion mutant lacking exon 8b was unstable, and another one lacking exons 8a and 8b (PML IVΔ8ab) was not efficiently expressed in L-G cells (see Fig. S4B and S4C in the supplemental material), we used L-G/MT-PU.1 cells expressing PML lacking exons 7a, 8a, and 8b (PML IVΔ7a8ab) for further analysis (Fig. 5D). In addition to losing the colocalization and transcriptional cooperation with PU.1, PMLΔ7a8ab had no effect on the profile of PU.1-induced C/EBPε expression and cell differentiation (compare Fig. 5E and S4D and S4E in the supplemental material with Fig. 4B, C, and E).

We also performed reciprocal experiments employing PU.1 mutants. Coimmunoprecipitation analysis using PU.1 deletion mutants showed that the acidic amino-acid-rich region (DE region) of the PU.1 transactivation domain is necessary for an association with PML IV (Fig. 6A) (see Fig. S5A in the supplemental material). As expected, PML IV could no longer recruit PU.1 lacking the DE region (PU.1ΔDE) to PODs in vivo (Fig. 6B, top), nor could it enhance PU.1ΔDE-mediated transcription, although PU.1ΔDE itself has a weak ability to enhance transcription (Fig. 6C, lanes 5 and 6). In agreement with these results, the expression of PU.1ΔDE did not effectively induce the expression of C/EBPε, and the overexpression of PML IV could not rescue the expression of C/EBPε (Fig. 6E, top) or significantly affect the differentiation of L-G cells (see Fig. S5D and S5E in the supplemental material).

To confirm the significance of the physical interaction between PU.1 and PML IV, we performed parallel experiments using a PU.1ΔPEST mutant that retains the ability to bind PML IV (see Fig. S5A in the supplemental material). In contrast to PU.1ΔDE, PML IV enhanced PU.1ΔPEST-mediated transcription to an extent similar to that of wild-type PU.1 (Fig. 6C, lanes 7 and 8). PML IV also enhanced C/EBPε expression in L-G/MT-PU.1ΔPEST cells, although it did not affect the time course of C/EBPε expression (Fig. 6E, bottom). This cooperation between PML IV and PU.1ΔPEST was also observed in the granulocytic differentiation of L-G cells (see Fig. S5H and S5I in the supplemental material). Interestingly we noticed that PU.1ΔPEST expression in PML IV-transduced cells was maintained at a high level even after 48 h of treatment of $ZnSO_4$ compared to mock-transduced cells. RT-PCR analysis revealed that mRNA expression of PU.1ΔPEST was equal in both cells (see Fig. S5J in the supplemental material). These results suggest that PML IV enhances PU.1ΔPEST expression by a posttranscriptional mechanism.

Taken together, these results demonstrate that the specific interaction between PU.1 and PML IV is involved in their abilities to promote granulocytic differentiation.

PML IV promotes the association of PU.1 and p300 during granulocytic differentiation to form complexes for active expression of C/EBPε. We next investigated the significance of the interaction of PU.1 and PML in regulating C/EBPε expression during granulocytic differentiation. In HL-60 cells, RA treatment immediately increased the expression of PU.1, PML, and p300 for 48 h (Fig. 7A), which thereafter decreased (data not shown). The expression of all PML isoforms increased evenly. C/EBPε expression markedly increased for 48 h, whereas C/EBPβ expression transiently increased and then returned to a level equal to that of untreated cells. To determine the interaction of the ternary complex of PU.1/PML/p300 on the *C/EBPε* promoter, ChIP analysis was performed (Fig. 7B). Upon RA treatment, promoter-associated PU.1 modestly increased, and PML association gradually increased. A rapid recruitment of p300 within 24 h of RA treatment, which may be mediated by promoter-bound RAR through an RA-responsive element (RARE), was followed by further accumulation after 48 h of treatment. Note that the amount of p300 that coimmunoprecipitated with PU.1 was only minimally detected in untreated HL-60 cells but significantly increased within 48 h by RA treatment, and this increase was proportional to the amount of PML coimmunoprecipitation rather than the amount of PU.1 itself (Fig. 7C). These results demonstrate that the ternary complex of PU.1/PML/p300 forms on the *C/EBPε* promoter and that the association of the complex increases in parallel to PML recruitment on the promoter during the early stage of granulocytic differentiation.

PU.1 alone induced C/EBPε expression, although relatively slowly, in L-G cells (Fig. 4E and 7D). An interesting finding is that C/EBPε expression was induced proportionally to p300 coimmunoprecipitation with PU.1. Another important finding is that the amount of p300 coimunnoprecipitation with PU.1 increased proportionally to the expression level of PML (Fig. 7D). These results suggest a scaffold function of PML in the association of PU.1 and p300. To confirm this, the association of these proteins was further examined by immunoprecipitation experiments using a transient expression system. Although the interaction between p300 and PU.1 is seemingly enhanced by the coexpression of PML IV (Fig. 7E, top panels, lanes 3 and 4), the coexpression of PML IV also increased PU.1 expression. These results raised the possibility that the increased coimmunoprecipitation of p300 may be due simply to an increased expression and availability of PU.1. To exclude this possibility, a reciprocal experiment was performed. Coimmunoprecipitation of PU.1 with p300 was not efficiently detected in the absence of PML IV but was easily observed when PML IV was coexpressed (Fig. 7E, middle panels, lanes 3 and 4). On the other hand, the coexpression of PU.1 did not affect the interaction between p300 and PML IV (Fig. 7E, bottom panels, lanes 3 and 4). These results suggest that the association of PU.1 and p300 is more labile than that of PML and p300 and support the data obtained in HL-60 cells showing that it can be stabilized by PML IV. We next performed immunofluorescence experiments to further confirm whether PU.1, p300, and PML form ternary complexes in vivo (Fig. 7F). Whereas both PU.1 and p300 localized throughout the nucleus, they were concentrated in PODs when PML IV was coexpressed. We then investigated the cooperation of PML IV and p300 in PU.1-induced transcription by luciferase reporter assays (Fig. 7G). PU.1 activation of the *C/EBPε* promoter was only slightly enhanced by the coexpression of p300 alone, but it was synergistically enhanced by the coexpression of PML IV and p300.

Notably, PU.1 was not efficiently recruited to abnormal nuclear aggregates of a sumoylation-deficient PML IV-3R mutant (see Fig. S6A in the supplemental material), even though PML IV-3R could still associate with PU.1 in immunoprecipitation experiments (data not shown). In contrast, p300 still efficiently colocalized with PML IV-3R. In agreement with its inability to recruit PU.1, PML IV-3R did

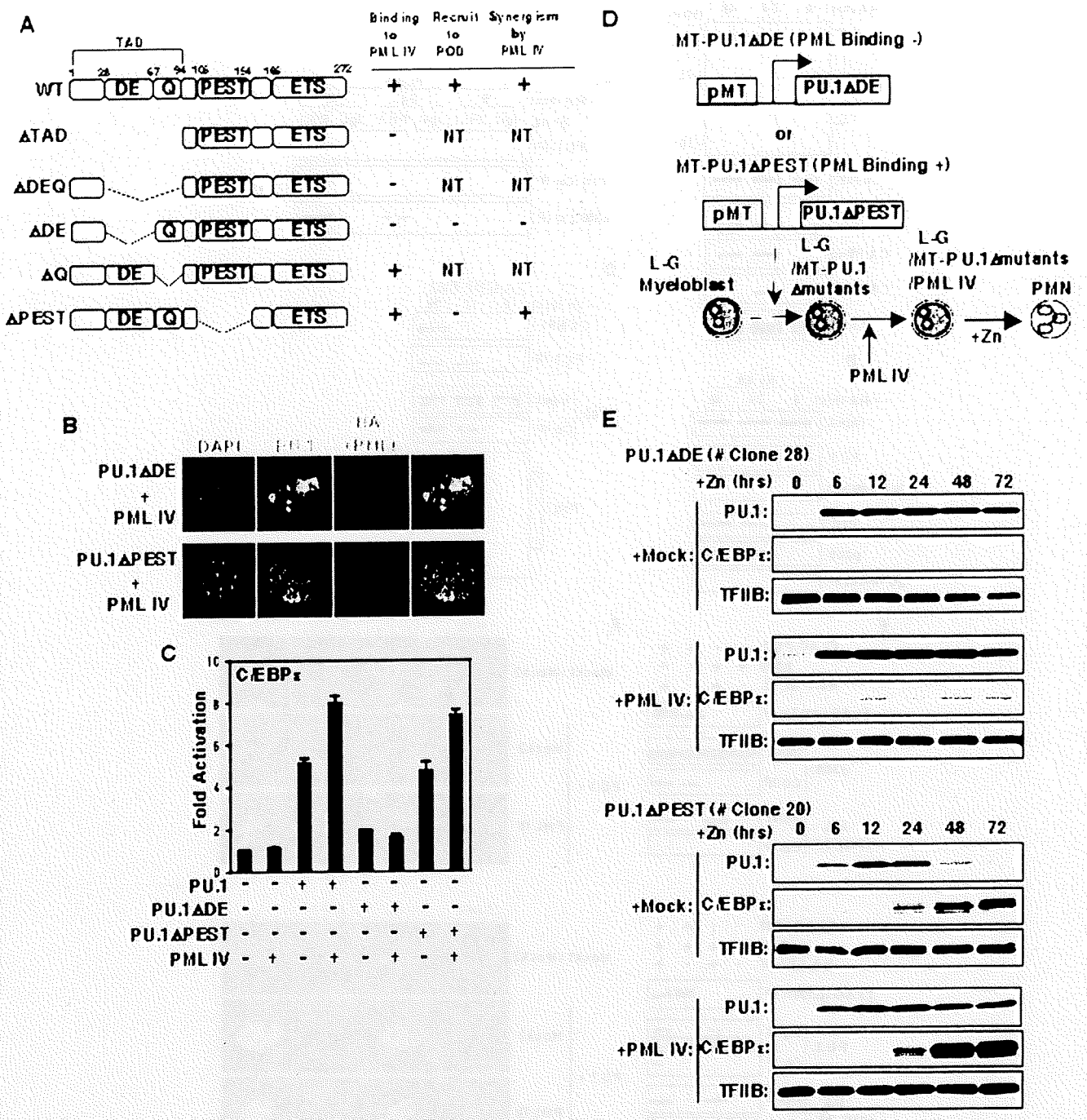

FIG. 6. The PU.1 transactivation subdomain is required for the enhancement of terminal differentiation by PML IV in L-G cells. (A) Schematics of PU.1 mutants and summary of the domain mapping of the physical and functional interaction with PML IV. TAD, transactivation domain; DE, acidic amino acid-rich region; Q, glutamine-rich region; ETS, *ets* DNA-binding domain; WT, wild type; NT, not tested. (B) Immunofluorescence shows that the PU.1 mutants do not colocalize with PML IV in NIH 3T3 cells. DAPI, 4′,6′-diamidino-2-phenylindole. (C) Luciferase reporter assays show that PML IV does not enhance the induction of transcription by the PU.1ΔDE. (D) Schematics of the L-G myeloblast clones transduced with mutant forms of PU.1. Those cells were further transduced with PML IV (L-G/MT-PU.1 Δmutants/PML IV) using a retroviral vector. (E) Western blots show that PML IV enhances the induction of C/EBPε expression by PU.1ΔPEST but not by PU.1ΔDE.

not enhance PU.1 transactivation (see Fig. S6B in the supplemental material). These results suggest that a normal POD structure would be crucial for transcriptional synergism between PU.1 and PML IV.

PML-RARA disrupts active PU.1/PML/p300 transcriptional ternary complex. We next tested whether PML-RARA can affect PU.1-induced transcription. The *C/EBPε* promoter contains RARE. We found that whereas ligand-unbound RARA

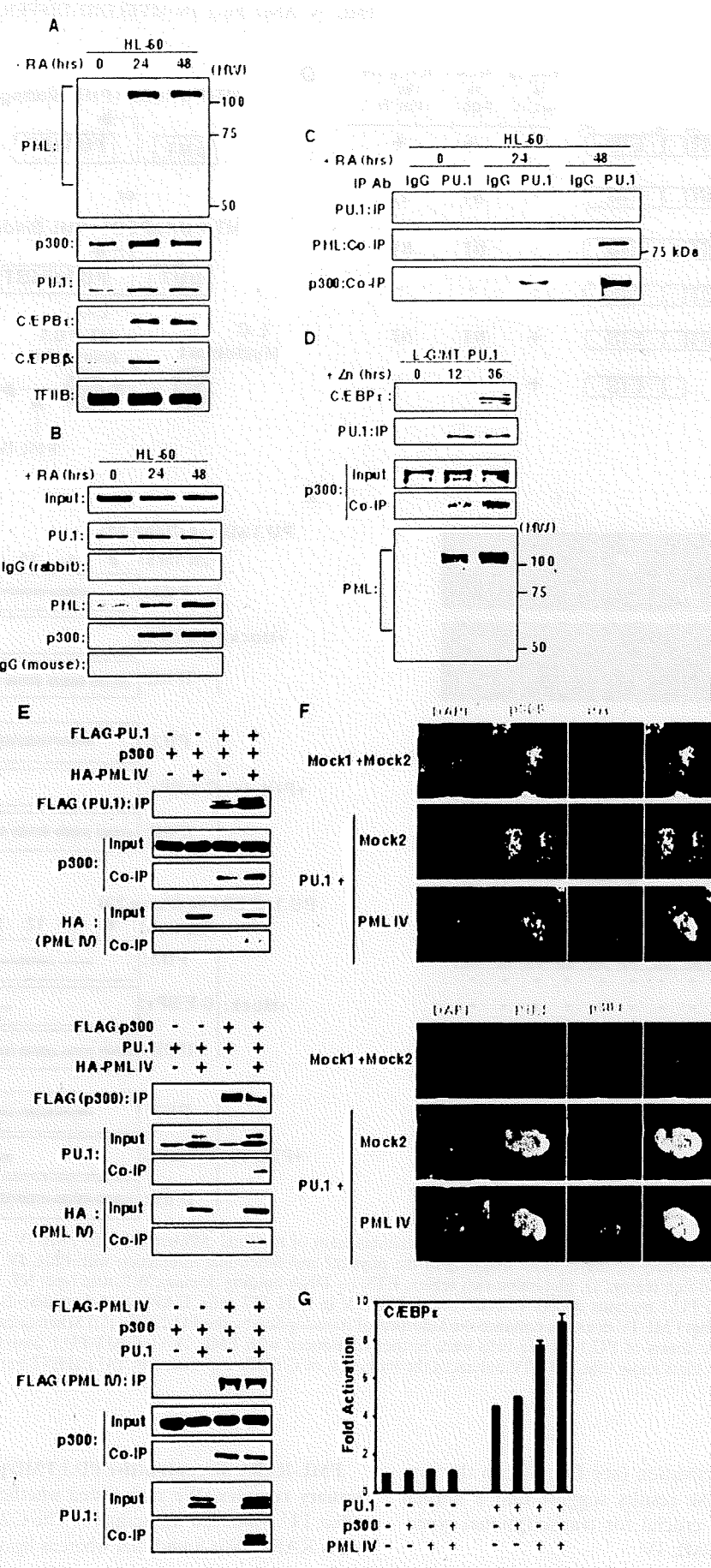

represses *C/EBPε* promoter activation, RA releases it to allow PU.1 to transactivate *C/EBPε* expression (see Fig. S7A in the supplemental material). PML-RARA also repressed promoter activity in the absence of RA (Fig. 8A). We also found that the enhancement of PU.1-induced transcription by PML IV was greatly reduced by the coexpression of a much lower amount of PML-RARA, suggesting its potent dominant-negative effect on PML IV. In addition, PML-RARA repressed the transactivation by PU.1 even in the absence of exogenous coexpression of PML IV.

To determine whether the direct recruitment of PML-RARA to the promoter is required for its inhibitory effect, we performed transactivation experiments using the RARE-mutated (*C/EBPε-mtRARE*) reporter to which PML-RARA could no longer bind. Neither PML-RARA nor the RARA/retinoid X receptor affected the reporter activity in the absence of RA (data not shown); however, PML-RARA still dose-dependently inhibited both PU.1 transactivation and the PML IV enhancement of PU.1-induced transcription, similar to the wild-type reporter (Fig. 8B). These results suggest that the inhibition of *C/EBPε* expression by PML-RARA is caused by the targeting of the PU.1-transcription factor complex. The *M-CSFR* promoter is also transrepressed by PML-RARA (data not shown), indicating that the effect of PML-RARA does not depend on the promoter context. Furthermore, PLZF-RARA, another APL-related chimera, disrupts the normal POD structure (20) and has effects that are similar to those of PML-RARA (see Fig. S7B in the supplemental material). These results suggest that the POD structure is required for PU.1 transactivation and is targeted by both chimeras.

To examine the inhibitory effects of PML-RARA on a different class of transcription factors, we performed parallel experiments using AML1b, which is functionally modulated by PML I (Fig. 8C). In contrast to its effects on PU.1, PML-RARA only partially attenuated the PML I enhancement of AML1b transcription. To exclude the possibility that the inhibitory action of PML-RARA is directed towards PML IV function, another parallel experiment was performed. c-Myb was also associated with and superactivated by PML IV but not markedly affected by PML-RARA (data not shown). These results indicate that PML-RARA specifically targets the interaction of PU.1 and PML IV.

We next considered the underlying mechanism for the differences in the effects of PML-RARA on PU.1 and AML1b. Immunoprecipitation experiments revealed that in PU.1 immunoprecipitates, the amount of p300 was remarkably reduced and that PML IV was lost when PML-RARA was coexpressed (Fig. 8D, top). In contrast, the coexpression of PML-RARA did not affect the amount of p300 coprecipitation but completely dissociated PU.1 from the PML IV immunoprecipitates (see Fig. S7C in the supplemental material). On the other hand, analysis of the AML1b complex revealed that the amount of p300 coprecipitation was not affected by the coexpression of PML I and/or PML-RARA (Fig. 8D, lower panels). The most striking difference was that PML-RARA coprecipitated with AML1b in the presence of PML I. Immunofluorescence analyses agreed with these results. PU.1 and AML1b were specifically colocalized in PML IV PODs and PML I PODs, respectively. When PML-RARA was coexpressed, the POD structures were disrupted, and PU.1 no longer colocalized with the PML IV microspeckles (Fig. 8E, top), whereas AML1b still colocalized with PML I microspeckles (Fig. 8E, bottom).

Finally, we examined the inhibition of PU.1-mediated granulocytic differentiation by PML-RARA in L-G/MT-PU.1 cells. The expression of PML-RARA in these cells (L-G/MT-PU.1/MT-PML-RARA) markedly suppressed PU.1-induced C/EBPε expression (Fig. 8F). The induction of PU.1 expression never reduced cell proliferation in those cells (data not shown). Morphological examination revealed that the expression of PML-RARA caused L-G cells to take on the appearance of APL cells and eliminated the ability of PU.1 to cause granulocytic differentiation, resulting in a premature arrest of differentiation (Fig. 8G).

DISCUSSION

In this study, we investigated the role of PML in myeloid differentiation and how the dominant-negative PML-RARA fusion affects the normal function of PML and gives rise to APL. Our results indicate the following: (i) PML cooperates with PU.1 to regulate C/EBPε expression during normal myeloid development, (ii) PML promotes the formation of an active transcription factor complex of PU.1 and p300 on the *C/EBPε* promoter during granulocytic differentiation, and (iii) PML-RARA has a dominant-negative effect not only on RA signaling but also on PML-induced transcription by disrupting the PU.1/PML/p300 ternary complex.

Role of PML in granuloid differentiation. PML is essential for RA action to induce terminal myeloid differentiation of precursor cells (32). On the other hand, the role of RA signaling during myeloid development is still controversial. Although C/EBPε is one of the most promising targets to help elucidate

FIG. 7. PML enhances the formation of the PU.1/p300 complex. (A) Expression of the PU.1/PML/p300 complex and selected C/EBP family members in HL-60 cells treated with RA for the indicated times. MW, molecular weight (in thousands). (B) PML and p300 are increasingly recruited onto the *C/EBPε* promoter in HL-60 cells treated with RA during the early stage of granulocytic differentiation. ChIP assays for region 2 were performed using antibodies as indicated. (C) The PU.1/p300 complex increases during RA-induced granulocytic differentiation. Lysates from HL-60 cells treated with RA for the indicated times were immunoprecipitated (IP) with an anti-PU.1 antibody (Ab), and coprecipitation of PML and p300 was analyzed by Western blotting. IgG, immunoglobulin G. (D) The PU.1/p300 complex increases along with PU.1 granulocytic differentiation. Lysates from L-G/MT-PU.1 cells treated with $ZnSO_4$ for the indicated time were immunoprecipitated with an anti-FLAG antibody (for PU.1 precipitation) and analyzed by Western blotting. The expression of C/EBPε and the PML protein is also shown. (E) Lysates from BOSC23 cells transfected with the indicated expression vectors were analyzed by immunoprecipitation with an anti-FLAG antibody and by Western blotting. (F) PML IV causes PU.1 and p300 to colocalize within PODs. Immunofluorescence was performed using anti-p300 and anti-PML (top) or an anti-PU.1 and anti-p300 (bottom) antibodies in NIH 3T3 cells transiently expressing PU.1 and PML IV. DAPI, 4′,6′-diamidino-2-phenylindole. (G) Functional relevance of PML IV effects on the PU.1/p300 complex. Luciferase assays using a reporter containing the *C/EBPε* promoter were performed using NIH 3T3 cells.

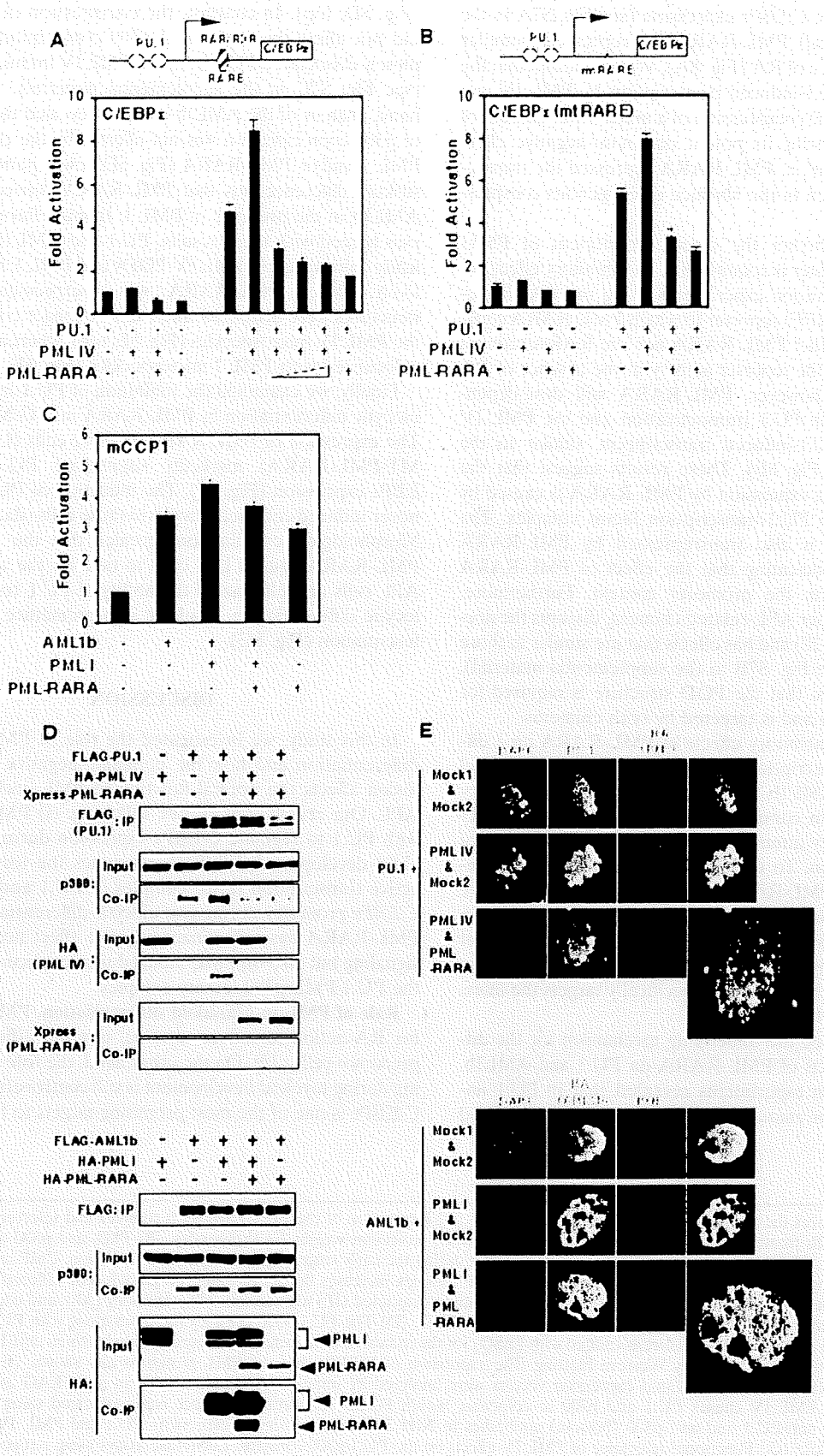

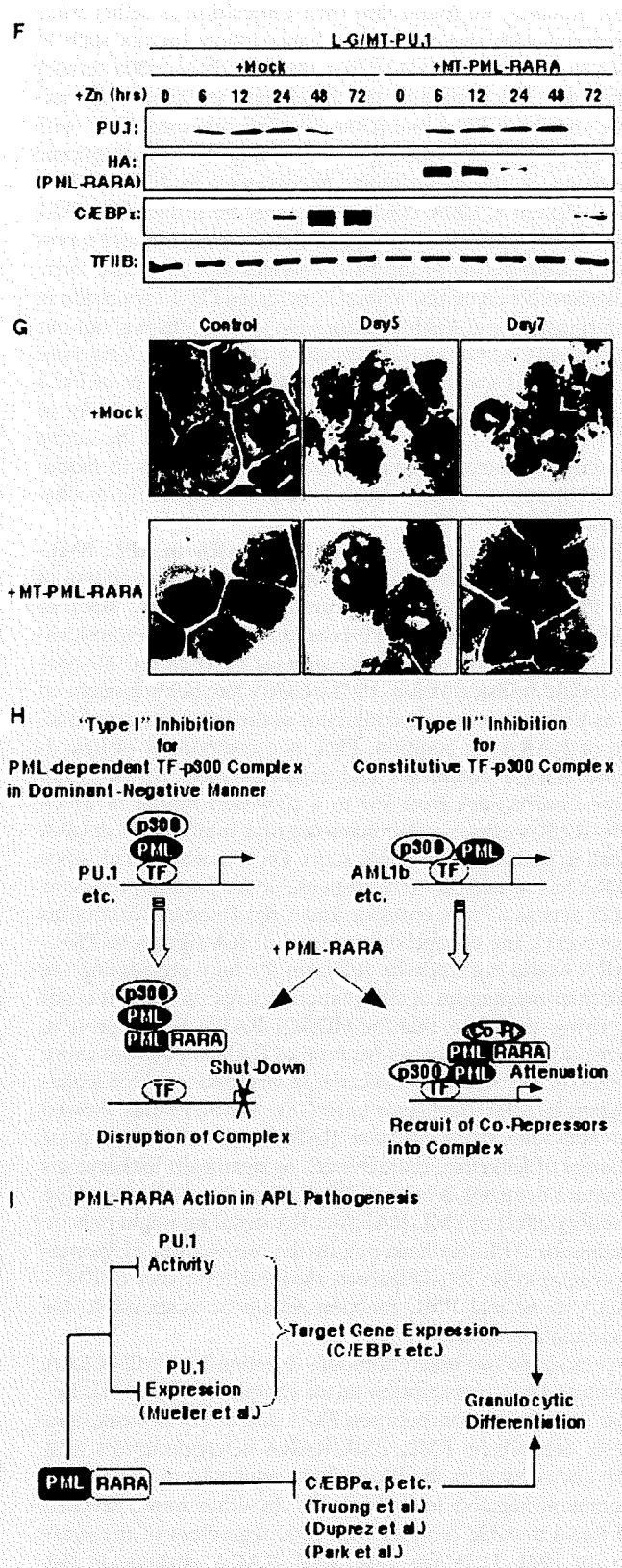

FIG. 8. PML-RARA disrupts PU.1/p300 complexes and prevents the enhancement of PU.1-induced C/EBPε expression by PML. (A) Luciferase assays in NIH 3T3 cells show that PML-RARA inhibits both the PU.1-mediated transactivation of *C/EBPε* and the enhancement of its transcription by PML IV in a dominant-negative fashion. (B) RARE is dispensable for PML-RARA-mediated inhibition of both PU.1- and PML IV-enhanced expression of *C/EBPε*. (C) PML-RARA has little effect on AML1b-mediated transcription. (D) PML-RARA disrupts the PML/PU.1/p300 complex but not the PML/AML1b/p300 complex. Lysates from BOSC23 cells transfected with the indicated expression vectors were immunoprecipitated (IP) with an anti-FLAG antibody and analyzed by Western blotting. Note that a 20-fold-longer exposure was needed to detect the coprecipitation of p300 with PU.1 than was needed to detect the coprecipitation with AML1b. (E) Differential effects of PML-RARA on the POD colocalization of transcription factors. PML-RARA disrupts PODs, resulting in APL-associated microspeckle structures. PU.1 was lost from these structures, whereas AML1b remained. DAPI, 4′,6′-diamidino-2-phenylindole. (F) Western blots show that PML-RARA potently suppressed the ability of PU.1 to induce C/EBPε expression in L-G cells. (G) PML-RARA potently suppresses PU.1-induced granulocytic differentiation of L-G cells according to morphological criteria. (H) Model of the inhibitory mechanisms of PML-RARA towards different classes of transcription factor complexes. In type I inhibition (e.g., for the PU.1 complex), PML-RARA has a dominant-negative effect. In contrast, in type II inhibition (e.g., for the AML1b complex), PML-RARA only attenuates the activity. (I) Model of PML-RARA-mediated differentiation arrest.

the RA action in granulopoiesis (23), *RARA*$^{-/-}$ mice normally express C/EBPε and show normal granulopoiesis. Rather, neutrophil differentiation occurs faster for BM cells derived from *RARA*$^{-/-}$ mice than for those derived from wild-type mice (11). These observations suggest that RARA is dispensable for granulopoiesis, and so the role of PML is other than to modulate the RA signaling. Granulopoiesis seems to be controlled by two pathways, at least in vitro, finally accompanying the increased expression of C/EBP families (37). Insufficient granulopoiesis observed in *PML*$^{-/-}$ mice would be explained by the redundancy of the process itself or that of C/EBPβ and C/EBPε function in addition to the regulatory rather than the mandatory function of PML. Contrary to data from a previous study (32), we found that immature granulocytes increase in BM of *PML*$^{-/-}$ mice. This discrepancy may be due to a different set of antibodies used for flow cytometry, which successfully revealed this subtle difference, which was undetected by the differential counts on cytospin smears.

Since PU.1 expression can induce L-G cells to differentiate into mature granulocytes without any additional cytokines, it is likely that PU.1 activates an unrevealed transcription cascade(s) that directs terminal differentiation in a cell-autonomous manner. Although the Pβ promoter contains RARE, and *C/EBPε* is upregulated by a pharmacological dose of RA, at least in vitro (23), RA treatment does not affect the DNase I hypersensitivity of Pβ (14). Those findings imply that a *trans*-acting factor(s) other than the RAR would control the chromatin structure. Another interesting finding is that RA fails to induce the expression of C/EBPε in C/EBPα-deficient cells (37), suggesting that a C/EBPα-initiating transcription cascade is responsible for RA signaling. Since PU.1 is one of the target genes induced by C/EBPα (31), it would be reasonable to speculate on the possible involvement of PU.1 in the regulation of *C/EBPε*. Taking our results of *C/EBPε* Pβ promoter analysis together with in vivo observations of *RARA*$^{-/-}$ mice (11), we propose a model that RAR would be a negative regulator to allow transcription upon RA binding and that

PU.1 should instead be considered an authentic transactivator for *C/EBPε* transcription that mediates the instructive role of PU.1 in granulocytic differentiation.

Elucidation of PML and PU.1 interaction during granulocytic differentiation. Although each PML isoform resides within discrete subnuclear compartments, there have been few reports on their innate biological activities in myeloid development. In this study, overexpression experiments were employed to delineate the function of each PML isoform. Because their protein expression levels could not be equalized, it might be possible that PML II, III, and V isoforms could not represent significant synergistic action with PU.1 simply due to their insufficient availability. In addition, since the expression level of transduced PML IV seems to be high compared to that of the endogenous one, the effect of PML IV on PU.1 action should be carefully interpreted. On the other hand, we think that PML overexpression employed in this study may mimic, at least in part, the increase of PML isoforms during the early stage of terminal granulocytic differentiation. We observed that PU.1 and PML mutually regulate each other. Although the mechanism remains unclear, we speculate that the increase of PML expression during RA-induced granulocytic differentiation might be due, at least in part, to an increase of PU.1 expression. Although the issue of isoform change during differentiation seems to be very important, we think at present that during granulocytic differentiation, PML (and PML IV) is regulated mainly quantitatively. In turn, PML IV specifically associates with PU.1 in vivo and enhances its function. Thus, PU.1 autoregulates its own transcriptional capability. The isoform-specific interaction was closely linked to the functional cooperation of PML and PU.1. Note that the ternary complex formation of PU.1/PML/p300 on the *C/EBPε* promoter depends on PML recruitment and that it occurs rapidly after RA treatment, suggesting its role at the early stage of granulocytic terminal differentiation.

On the other hand, the relevance of the POD structure to transcriptional control remains elusive. Sumoylation of PML IV is a prerequisite for the normal architecture of PODs (39) and seems to be crucial for the transcriptional regulation of the PU.1/PML/p300 complex. Furthermore, the B boxes and coiled-coil domain of PML, essential for the formation of the normal POD structure, were required for the colocalization of PU.1 with PML IV. We also observed that PML VI cannot efficiently associate with PU.1 but does recruit it to PODs, and this activity is correlated with the cooperation of these proteins in the granulocytic differentiation of L-G cells, although PML VI does so less efficiently than PML IV. We speculate that PML VI indirectly regulates PU.1; e.g., PML VI may promote PML IV-mediated PU.1 targeting to PODs, although a complete understanding of the interaction between PML isoforms remains challenging. Another interesting finding is that PML IV augmented only the amount of C/EBPε expression but did not affect its time course profile in L-G cells expressing PU.1ΔPEST. Taken together with the finding that PU.1ΔPEST could not be efficiently recruited to PODs, we believe at present that PML IV-mediated ternary complex formation within the structurally integrated PODs would be required for the synergistic activation of transcription by the PU.1/PML/p300 ternary complex in vivo.

PU.1 and p300/CBP can directly interact, at least in vitro (33); however, we found that their association is rather weak compared with those of other transcription factors such as AML1b. We demonstrated that the PU.1/PML/p300 ternary complex is also formed on the target gene promoter and speculate that both PU.1 and p300 are efficiently assembled with the aid of PML IV, leading to the synergistic transcriptional activation of the target gene. As observed in LG/MT-PU.1 cells, efficient C/EBPε expression cannot be induced by PU.1 alone but requires the increase of PML expression and a possible reorganization of the PU.1 complex into an active form.

We also observed that PML IV increases PU.1 expression in both transient and stable coexpression systems throughout our experiments. Although its molecular mechanism remains to be elucidated, we speculate that the PML enhancement of PU.1 activity has an additional aspect of increased availability of PU.1 in addition to promoting the formation of the active transcription factor complex. Thus, PML IV seems to modulate PU.1 activity by both qualitative and quantitative mechanisms.

Reconsideration of the role of PML-RARA in APL: PML-RARA as a dominant-negative mutant causing dissociation of the PML-mediated transcription factor complex. Because RARA is a target for all APL-related chromosomal translocations, an alteration of its function must be required for promyelocytic transformation. PML-RARA has been thought to act as a dominant-negative inhibitor of the transactivator function of RARA. In addition, PML is a component of ligand-bound RARA complexes and regulates their activity (38). These observations have led to a proposed model in which PML-RARA acts as a dominant-negative inhibitor of the RA signaling pathway at multiple steps. On the other hand, since RARA has turned out to be dispensable for granulopoiesis, or rather acts as a transrepressor under physiological conditions in vivo (11), the enhanced repression of RA signals by PML-RARA would not likely be sufficient for fully elucidating the molecular mechanism of differentiation arrest in APL. It is not surprising, therefore, that the HDAC1-RARA fusion protein, a bona fide dominant-negative form of RARA, does not cause a block in myeloid differentiation in vivo and was not leukemogenic in those transgenic mice (18). Another study showed that homodimerizing artificial RAR fusions alone are poor initiators of leukemia, characterized by significant leukocytosis of mature neutrophils in vivo (28). Rather, the main role of the inhibitory effect of PML-RARA in RA signaling might only be priming for APL-like leukemia by the attenuation of spontaneous apoptosis (15). Therefore, the inhibitory roles of PML-RARA in normal PML function should be responsible for differentiation arrest.

We propose two different modes of action for PML-RARA inhibiting PML/transcription factor complexes (Fig. 8H). Because the association between PU.1 and p300 is weak, and largely depends on PML, PML-RARA heterodimerizes with PML and sequesters the PML/p300 complex from PU.1 (type I dominant-negative inhibition). On the other hand, AML1b still forms a stable complex with p300 regardless of the presence of PML I. In this case, PML-RARA gathers on the AML1b/p300 complex through heterodimerization with PML I and then attenuates the transcriptional activity, probably by recruiting corepressor complexes to overcome the histone acetyltransferase activity of p300/CBP (type II inhibition).

Thus, the inhibitory effects of PML-RARA would depend largely on the stability of a given transcription factor/p300 complex for PML.

Several lines of evidence suggest roles for C/EBPε in APL pathogenesis. Differentiation of BM cells from *C/EBPε*$^{-/-}$ mice is practically arrested at the promyelocyte stage, at least in vitro (34a). In addition, a previous excellent study shows that the overexpression of C/EBPε in APL rescues differentiation arrest in vitro as well as in vivo and prolongs the survival of mice transplanted with APL cells (29). On the other hand, repression of C/EBPε does not fully account for the pathophysiology of APL, because *C/EBPε*$^{-/-}$ mice do not capture the APL phenotype. Walter et al. previously reported that reduced PU.1 expression causes myeloid progenitor expansion and increased leukemia penetrance in mice expressing PML-RARA (30). Those authors also demonstrated that PML-RARA decreases the expression of PU.1 mRNA in PU.1-haploinsuficient mice by unknown mechanisms, causing the development of a hypomorphic PU.1 phenotype. Because PU.1 autoregulates its own expression (1), our results showing that PML-RARA inhibits the transcriptional capability of PU.1 agree with their findings and might partly explain the graded reduction of physiological PU.1 below a critical level, followed by the induction of myeloid leukemia (26). Thus, we suppose that the repression of PU.1 is one of the crucial mechanisms in PML-RARA leukemogenesis. Furthermore, PML-RARA is a multivalent suppressor for other C/EBP family members, including C/EBPα and C/EBPβ (4, 24, 29). We think that comprehensive inhibition of those transcription factors might be responsible for the full manifestation of APL.

There are four other types of APL-related chimeras that have been reported. Among them, NPM- or NuMA-RARA fusions do not affect the POD structure (8). In this respect, PML localization itself is not of primary importance for APL pathogenesis. On the other hand, disruption of the POD structure into microspeckles is invariably observed in t(15;17)-bearing APL, and the restoration of normal POD architecture is an early event in granulocytic differentiation following RA-induced degradation of PML-RARA (35). Therefore, POD structure-based PML function still seems to be a key target for the pathogenesis of PML-RARA-induced APL.

ACKNOWLEDGMENTS

We thank Francoise Moreau-Gachelin (INSERM, France), Zu Chen (Shanghai Institute of Hematology, People's Republic of China), Akira Kakizuka (Kyoto University, Japan), and Pierre Chambon (INSERM, France) for kindly providing the cDNAs for PU.1, PLZF-RARA, PML-RARA, and RAR and retinoid X receptor, respectively. We also thank Kimiko Shimizu and Kazutsune Yamagata for supervision of the ChIP assay and Chikako Hatanaka and Noriko Aikawa for technical assistance.

This work was supported in part by a grant-in-aid from the Japanese Ministry of Education, Culture, Sports, and Science and by a grant from the Leukemia Study Group of the Ministry of Health, Labor, and Welfare.

REFERENCES

1. **Chen, H., D. Ray-Gallet, P. Zhang, C. J. Hetherington, D. A. Gonzalez, D. Zhang, F. Moreau-Gachelin, and D. G. Tenen.** 1995. PU.1 (Spi-1) autoregulates its expression in myeloid cells. Oncogene **11**:1549–1560.
2. **Chumakov, A. M., I. Grillier, E. Chumakov, D. Chih, J. Slater, and H. P. Koeffler.** 1997. Cloning of the novel human myeloid-cell-specific C/EBP-epsilon transcription factor. Mol. Cell. Biol. **17**:1375–1386.
3. **de The, H., C. Lavau, A. Marchio, C. Chomienne, L. Degos, and A. Dejean.** 1991. The PML-RAR alpha fusion mRNA generated by the t(15;17) translocation in acute promyelocytic leukemia encodes a functionally altered RAR. Cell **66**:675–684.
4. **Duprez, E., K. Wagner, H. Koch, and D. G. Tenen.** 2003. C/EBPβ: a major PML-RARA-responsive gene in retinoic acid-induced differentiation of APL cells. EMBO J. **22**:5806–5816.
5. **Fisher, R. C., and E. W. Scott.** 1998. Role of PU.1 in hematopoiesis. Stem Cells **16**:25–37.
6. **Friedman, A. D.** 2002. Transcriptional regulation of granulocyte and monocyte development. Oncogene **21**:3377–3390.
7. **Gombart, A. F., S. H. Kwok, K. Anderson, Y. Yamaguchi, B. E. Torbett, and H. P. Koeffler.** 2003. Regulation of neutrophil and eosinophil secondary granule gene expression by transcription factors C/EBP epsilon and PU.1. Blood **101**:3265–3273.
8. **Grimwade, D., A. Biondi, M. J. Mozziconacci, A. Hagemeijer, R. Berger, M. Neat, K. Howe, N. Dastugue, J. Jansen, I. Radford-Weiss, F. Lo Coco, M. Lessard, J. M. Hernandez, E. Delabesse, D. Head, V. Liso, D. Sainty, G. Flandrin, E. Solomon, F. Birg, M. Lafage-Pochitaloff, et al.** 2000. Characterization of acute promyelocytic leukemia cases lacking the classic t(15;17): results of the European Working Party. Blood **96**:1297–1308.
9. **Jensen, K., C. Shiels, and P. S. Freemont.** 2001. PML protein isoforms and the RBCC/TRIM motif. Oncogene **20**:7223–7233.
10. **Kakizuka, A., W. H. Miller, Jr., K. Umesono, R. P. Warrell, Jr., S. R. Frankel, V. V. Murty, E. Dmitrovsky, and R. M. Evans.** 1991. Chromosomal translocation t(15;17) in human acute promyelocytic leukemia fuses RAR alpha with a novel putative transcription factor, PML. Cell **66**:663–674.
11. **Kastner, P., and S. Chan.** 2001. Function of RARalpha during the maturation of neutrophils. Oncogene **20**:7178–7185.
12. **Kastner, P., H. J. Lawrence, C. Waltzinger, N. B. Ghyselinck, P. Chambon, and S. Chan.** 2001. Positive and negative regulation of granulopoiesis by endogenous RARalpha. Blood **97**:1314–1320.
13. **Klemsz, M. J., S. R. McKercher, A. Celada, C. Van Beveren, and R. A. Maki.** 1990. The macrophage and B cell-specific transcription factor PU.1 is related to the ets oncogene. Cell **61**:113–124.
14. **Kubota, T., T. Hirama, W. Verbeek, S. Kawano, D. Y. Chih, A. M. Chumakov, H. Taguchi, and H. P. Koeffler.** 2001. DNase I hypersensitivity analysis of the human CCAAT enhancer binding protein epsilon (C/EBPepsilon) gene. Leuk. Res. **25**:981–995.
15. **Kuwata, T., I. M. Wang, T. Tamura, R. M. Ponnamperuma, R. Levine, K. L. Holmes, H. C. Morse, L. M. De Luca, and K. Ozato.** 2000. Vitamin A deficiency in mice causes a systemic expansion of myeloid cells. Blood **95**: 3349–3356.
16. **Lee, K. H., T. Kinashi, K. Tohyama, K. Tashiro, N. Funato, K. Hama, and T. Honjo.** 1991. Different stromal cell lines support lineage-selective differentiation of the multipotential bone marrow stem cell clone LyD9. J. Exp. Med. **173**:1257–1266.
17. **Lekstrom-Himes, J. A.** 2001. The role of C/EBPε in the terminal stages of granulocyte differentiation. Stem Cells **19**:125–133.
18. **Matsushita, H., P. P. Scaglioni, M. Bhaumik, E. M. Rego, L. F. Cai, S. M. Majid, H. Miyachi, A. Kakizuka, W. H. Miller, Jr., and P. P. Pandolfi.** 2006. In vivo analysis of the role of aberrant histone deacetylase recruitment and RAR alpha blockade in the pathogenesis of acute promyelocytic leukemia. J. Exp. Med. **203**:821–828.
19. **McKercher, S. R., B. E. Torbett, K. L. Anderson, G. W. Henkel, D. J. Vestal, H. Baribault, M. Klemsz, A. J. Feeney, G. E. Wu, C. J. Paige, and R. A. Maki.** 1996. Targeted disruption of the PU.1 gene results in multiple hematopoietic abnormalities. EMBO J. **15**:5647–5658.
20. **Melnick, A., and J. D. Licht.** 1999. Deconstructing a disease: RARalpha, its fusion partners, and their roles in the pathogenesis of acute promyelocytic leukemia. Blood **93**:3167–3215.
21. **Nguyen, L. A., P. P. Pandolfi, Y. Aikawa, Y. Tagata, M. Ohki, and I. Kitabayashi.** 2005. Physical and functional link of the leukemia-associated factors AML1 and PML. Blood **105**:292–300.
22. **Olson, M. C., E. W. Scott, A. A. Hack, G. H. Su, D. G. Tenen, H. Singh, and M. C. Simon.** 1995. PU.1 is not essential for early myeloid gene expression but is required for terminal myeloid differentiation. Immunity **3**:703–714.
23. **Park, D. J., A. M. Chumakov, P. T. Vuong, D. Y. Chih, A. F. Gombart, W. H. Miller, Jr., and H. P. Koeffler.** 1999. CCAAT/enhancer binding protein epsilon is a potential retinoid target gene in acute promyelocytic leukemia treatment. J. Clin. Investig. **103**:1399–1408.
24. **Park, D. J., P. T. Vuong, S. de Vos, D. Douer, and H. P. Koeffler.** 2003. Comparative analysis of genes regulated by PML/RAR alpha and PLZF/RAR alpha in response to retinoic acid using oligonucleotide arrays. Blood **102**:3727–3736.
25. **Piazza, F., C. Gurrieri, and P. P. Pandolfi.** 2001. The theory of APL. Oncogene **20**:7216–7222.
26. **Rosenbauer, F., K. Wagner, J. L. Kutok, H. Iwasaki, M. M. Le Beau, Y. Okuno, K. Akashi, S. Fiering, and D. G. Tenen.** 2004. Acute myeloid leukemia induced by graded reduction of a lineage-specific transcription factor, PU.1. Nat. Genet. **36**:624–630.
27. **Scott, E. W., M. C. Simon, J. Anastasi, and H. Singh.** 1994. Requirement of

transcription factor PU.1 in the development of multiple hematopoietic lineages. Science 265:1573–1577.
28. **Sternsdorf, T., V. T. Phan, M. L. Maunakea, C. B. Ocampo, J. Sohal, A. Silletto, F. Galimi, M. M. Le Beau, R. M. Evans, and S. C. Kogan.** 2006. Forced retinoic acid receptor alpha homodimers prime mice for APL-like leukemia. Cancer Cell 9:81–94.
29. **Truong, B. T., Y. J. Lee, T. A. Lodie, D. J. Park, D. Perrotti, N. Watanabe, H. P. Koeffler, H. Nakajima, D. G. Tenen, and S. C. Kogan.** 2003. CCAAT/enhancer binding proteins repress the leukemic phenotype of acute myeloid leukemia. Blood 101:1141–1148.
30. **Walter, M. J., J. S. Park, R. E. Ries, S. K. Lau, M. McLellan, S. Jaeger, R. K. Wilson, E. Mardis, and T. J. Ley.** 2005. Reduced PU.1 expression causes myeloid progenitor expansion and increased leukemia penetrance in mice expressing PML-RARalpha. Proc. Natl. Acad. Sci. USA 102:12513–12518.
31. **Wang, X., E. Scott, C. L. Sawyers, and A. D. Friedman.** 1999. C/EBPα bypasses granulocyte colony-stimulating factor signals to rapidly induce PU.1 gene expression, stimulates granulocyte differentiation and limit proliferation in 32Dcl3 myeloblasts. Blood 94:560–571.
32. **Wang, Z. G., L. Delva, M. Gaboli, R. Rivi, M. Giorgio, C. Cordon-Cardo, F. Grosveld, and P. P. Pandolfi.** 1998. Role of PML in cell growth and the retinoic acid pathway. Science 279:1547–1551.
33. **Yamamoto, H., F. Kihara-Negishi, T. Yamada, Y. Hashimoto, and T. Oikawa.** 1999. Physical and functional interactions between the transcription factor PU.1 and the coactivator CBP. Oncogene 18:1495–1501.
34. **Yamanaka, R., G. D. Kim, H. S. Radomska, J. Lekstrom-Himes, L. T. Smith, P. Antonson, D. G. Tenen, and K. G. Xanthopoulos.** 1997. CCAAT/enhancer binding protein epsilon is preferentially up-regulated during granulocytic differentiation and its functional versatility is determined by alternative use of promoters and differential splicing. Proc. Natl. Acad. Sci. USA 94:6462–6467.
34a. **Yamanaka, R., C. Barlow, J. Lekstrom-Himes, L. H. Castilla, P. P. Liu, M. Eckhaws, T. Decker, A. Wynshaw-Boris, and K. G. Xanthopoulos.** 1997. Impaired granulopoiesis, myelodysplasia, and early lethality in CCAAT/enhancer binding protein epsilon-deficient mice. Proc. Natl. Acad. Sci. USA 94:13187–13192.
35. **Yoshida, H., K. Kitamura, K. Tanaka, S. Omura, T. Miyazaki, T. Hachiya, R. Ohno, and T. Naoe.** 1996. Accelerated degradation of PML-retinoic acid receptor alpha (PML-RARA) oncoprotein by all-trans-retinoic acid in acute promyelocytic leukemia: possible role of the proteasome pathway. Cancer Res. 56:2945–2948.
36. **Zelent, A., F. Guidez, A. Melnick, S. Waxman, and J. D. Licht.** 2001. Translocations of the RARalpha gene in acute promyelocytic leukemia. Oncogene 20:7186–7203.
37. **Zhang, P., E. Nelson, H. S. Radomska, J. Iwasaki-Arai, K. Akashi, A. D. Friedman, and D. G. Tenen.** 2002. Induction of granulocytic differentiation by 2 pathways. Blood 99:4406–4412.
38. **Zhong, S., L. Delva, C. Rachez, C. Cenciarelli, D. Gandini, H. Zhang, S. Kalantry, L. P. Freedman, and P. P. Pandolfi.** 1999. A RA-dependent, tumour-growth suppressive transcription complex is the target of the PML-RARalpha and T18 oncoproteins. Nat. Genet. 23:287–295.
39. **Zhong, S., S. Muller, S. Ronchetti, P. Freemont, A. Dejean, and P. P. Pandolfi.** 2000. Role of SUMO-1-modified PML in nuclear body formation. Blood 95:2748–2753.
40. **Zhong, S., P. Salomoni, and P. P. Pandolfi.** 2000. The transcriptional role of PML and the nuclear body. Nat. Cell Biol. 5:85–90.

MOLECULAR AND CELLULAR BIOLOGY, Nov. 2007, p. 7649–7660 Vol. 27, No. 21
0270-7306/07/$08.00+0 doi:10.1128/MCB.01246-07

CUB Domain-Containing Protein 1 Is a Novel Regulator of Anoikis Resistance in Lung Adenocarcinoma▽†

Takamasa Uekita,[1] Lin Jia,[1] Mako Narisawa-Saito,[2] Jun Yokota,[3] Tohru Kiyono,[2] and Ryuichi Sakai[1]*

Growth Factor Division,[1] Virology Division,[2] and Biology Division,[3] National Cancer Center Research Institute, 5-1-1 Tsukiji, Chuo-ku, Tokyo 104-0045, Japan

Received 12 July 2007/Returned for modification 31 July 2007/Accepted 16 August 2007

Malignant tumor cells frequently achieve resistance to anoikis, a form of apoptosis induced by detachment from the basement membrane, which results in the anchorage-independent growth of these cells. Although the involvement of Src family kinases (SFKs) in this alteration has been reported, little is known about the signaling pathways involved in the regulation of anoikis under the control of SFKs. In this study, we identified a membrane protein, CUB-domain-containing protein 1 (CDCP1), as an SFK-binding phosphoprotein associated with the anchorage independence of human lung adenocarcinoma. Using RNA interference suppression and overexpression of CDCP1 mutants in lung cancer cells, we found that tyrosine-phosphorylated CDCP1 is required to overcome anoikis in lung cancer cells. An apoptosis-related molecule, protein kinase Cδ, was found to be phosphorylated by the CDCP1-SFK complex and was essential for anoikis resistance downstream of CDCP1. Loss of CDCP1 also inhibited the metastatic potential of the A549 cells in vivo. Our findings indicate that CDCP1 is a novel target for treating cancer-specific disorders, such as metastasis, by regulating anoikis in lung adenocarcinoma.

Src family kinases (SFKs) play important roles in various cell functions, including cell proliferation, cell adhesion, and cell migration, under the control of extracellular stimuli (26). Many studies have shown elevated activity of SFKs or increased protein expression in a variety of human cancers (31). The activities of SFKs often correlate with the malignant potential of cancer and poor prognosis (36). SFKs may contribute to various aspects of tumor progression, including uncontrolled proliferation and migration, disruption of cell-cell contacts, invasiveness, angiogenesis, and resistance to apoptosis.

Anoikis is a form of apoptosis triggered by the loss of cell survival signals generated from interaction with the extracellular matrix (10). Anoikis is considered to be physiologically important in the maintenance of homeostasis and tissue architecture (24). On the other hand, the resistance to anoikis acquired during carcinogenesis has been described as a core aspect of cancer cells for tumor progression and metastasis (12). This property indicates the existence of survival signals in tumor cells, which compensate for similar signals supported by cell-matrix interactions. Since they were originally described by Frisch and Francis (9), several previous reports have shown the crucial role of SFKs in the anoikis resistance of tumor cells. Viral Src oncoprotein abrogates anoikis in epithelial cells (13). Src activation is also important for resistance to anoikis in various cancers, such as colon tumor and lung adenocarcinoma cells (33, 35). However, the exact mechanism that is responsible for the anoikis resistance mediated by SFKs in human cancer cells has not been clearly elucidated.

The purpose of this study, therefore, was to identify the key molecules of anoikis resistance, which mediate signals from activated SFKs in human cancer cells. For that purpose, we analyzed proteins binding to SFKs with and without cell attachment in a number of human lung cancer cell lines. We found that tyrosine phosphorylation of a 135-kDa SFK-binding protein is associated with elevated anchorage independence in a group of lung cancer cell lines, especially in a cell suspension condition. This 135-kDa phosphoprotein was purified and identified as CUB-domain-containing protein 1 (CDCP1) by mass spectrometry. The protein CDCP1 is a type I transmembrane protein that has possible roles in cell-cell and cell-matrix adhesion (3, 5). The molecule has been reported to be highly expressed in lung, breast, and colon cancers (6, 28). Using an RNA interference (RNAi) technique, it was determined that CDCP1 is required for the survival of lung cancer cells both in suspension culture and in soft agar. This study identifies a novel modulator that sustains anoikis resistance under the control of SFKs in lung cancer cells.

MATERIALS AND METHODS

Plasmids, antibodies, and reagents. Full-length cDNA of human CDCP1 with a FLAG tag at the C terminus (wild type [WT]) was obtained by reverse transcription-PCR amplification from the mRNA of A549 human lung adenocarcinoma cells and cloned into pcDNA3.1 (Invitrogen). The cytoplasmic-domain mutants of CDCP1, Y734F (Tyr734 to Phe), Y762F (Tyr762 to Phe), and Y2F (Y734 and Y762 double mutant), were generated by PCR using the overlap extension method of Ho et al. (14). The C2 domain of protein kinase Cδ (PKCδ) corresponding to amino acids (1 to 160) with a hemagglutinin (HA) tag at the C terminus was obtained by PCR and cloned into pcDNA3.1 (Invitrogen). To express the Fyn Src homology 2 (SH2) domain fused with glutathione *S*-transferase (GST) protein (GST-FynSH2), a cDNA fragment of the Fyn SH2 domain corresponding to nucleotides 1018 to 1299 of the reported sequence (GenBank accession number NM_002037) was amplified by PCR and cloned into pGEX4T2 (Amersham Pharmacia).

Antiphosphotyrosine antibody (4G10) and anti-c-Src antibody (clone GD11) were purchased from Upstate Biotechnology. Anti-Akt antibody, anti-phospho-Akt (Ser473) antibody, anti-ERK1/2 antibody (p44/p42 mitogen-activated protein kinase [MAPK] antibody), anti-phospho-ERK1/2 antibody (phospho-p44/p42 MAPK [Thr202/Tyr204] antibody), anti-p38MAPK antibody, anti-phospho-

* Corresponding author. Mailing address: Growth Factor Division, National Cancer Center Research Institute, 5-1-1 Tsukiji, Chuo-ku, Tokyo 104-0045, Japan. Phone: 81-3-3547-5247. Fax: 81-3-3542-8170. E-mail: rsakai@gan2.res.ncc.go.jp.

† Supplemental material for this article may be found at http://mcb.asm.org/.

▽ Published ahead of print on 4 September 2007.

p38MAPK (Thr180/Tyr182) antibody, and anti-phospho-PKCδ (Tyr311) antibody were purchased from Cell Signaling. Anti-HA (Y-11), anti-PKCδ (C-20), and anti-Fyn (FYN3) antibodies were purchased from Santa Cruz Biotechnology. Anti-FLAG antibody (Anti-FLAG M2 peroxidase conjugate specific antibody) and antitubulin antibody (clone B-5-1-2) were purchased from Sigma. The anti-c-Yes antibody was purchased from Transduction Laboratories. An anti-CDCP1 antibody (ab1377) was purchased from Abcam Ltd. To generate the CDCP1 antibody, anti-CDCP1 and the anti-phospho-CDCP1 (Tyr734) antibody were obtained by rabbit immunization using the cytoplasmic domain of CDCP1 fused to GST, and the amino peptides NDSHV(pY^{734})AVIEC of CDCP1 were obtained from MBL Co., Ltd. Horseradish peroxidase (HRP)-conjugated anti-mouse and anti-rabbit antibodies were purchased from Amersham Pharmacia. The HRP-conjugated anti-goat immunoglobulin G (IgG) antibody was purchased from ZYMED. Mouse, rabbit, and goat IgGs were purchased from DakoCytomation. The SFK inhibitor PP2 and the structural analog PP3 were purchased from Calbiochem-Novabiochem Ltd. Etoposide and Rottlerin were purchased from Sigma-Aldrich.

Cell culture and transfection. The human lung adenocarcinoma cell lines A549, PC14, and H322 and human lung squamous carcinoma cell lines H520 and H157 were maintained in RPMI 1640 medium with 10% fetal bovine serum (FBS) at 37°C with 5% CO_2. For transfection, cells were seeded on a cell culture plate or a 2-methacryloyloxyethyl phosphorylcholine (MPC)-coated plate (Nunc) at 1.5×10^5 cells per six wells or 9.0×10^5 cells/10-cm plate, and transfection was performed after 14 h. Expression plasmids were transfected by Lipofectamine 2000 (Invitrogen) according to the manufacturer's instructions. To investigate the effect of PP2 treatment, cells were treated with 10 μM of PP2 or 10 μM of PP3.

Construction of dicer, stealth siRNAs, and miR RNAi vectors. Dicer small interfering RNAs (siRNAs) of human c-Src, Fyn, and c-Yes were generated using the BLOCK-iT RNAi TOPO transcription kit and BLOCK-iT complete dicer RNAi kit (Invitrogen) according to the manufacturer's instructions. In the generation of siRNA for Src, a 726-bp fragment from the initiation codon of human c-Src was chosen as the target sequence and amplified by PCR using the primers forward, 5′-ATGGGTAGCAACAAGAGCAAG-3′, and reverse, 5′-GTGGCACAGGCCATCGGCGTG-3′. As for Fyn and c-Yes, 999-bp and 857-bp fragments were chosen as the target sequences, respectively, and amplified with the following primers: Fyn forward, 5′-ATGGGCTGTGTGCAATGTAGG-3′, and reverse, 5′-CACCACTGCATAGAGCTGGAC-3′; c-Yes forward, 5′-CTGAAAATACTCCAGAGCCTG-3′, and reverse, 5′-CTTTGTCCTAGTTTAACCTCTAG-3′. Dicer siRNA of LacZ was generated by the same procedure as dicer siRNAs of c-Src, Fyn, and c-Yes and was used as a negative control. The stealth siRNAs of human CDCP1, PKCδ, and the negative control were ordered from Invitrogen. Specific primers were as follows: CDCP1 forward, 5′-GCUCUGCCACGAGAAAGCAACAUUA-3′, and reverse, 5′-UAAUGUUGCUUUCUCGUGGCAGAGC-3′; PKCδ forward, 5′-GGUGCAGAAGAAGCCGACCAUGUAU-3′, and reverse, 5′-AUACAUGGUCGGCUUCUUCUGCACC-3′. Transfection of both dicer and stealth siRNAs was performed with Lipofectamine 2000 (Invitrogen), and the effect was analyzed less than 48 h after the transfection.

A system stably expressing siRNA was generated using the BLOCK-iT Pol II miR RNAi expression vector kit (Invitrogen) according to the manufacturer's instructions. In the generation of the miR RNAi vector for humans, CDCP1 was chosen as the target sequence, using the forward primer 5′-TGCTGAATGTTGCTTTCTCGTGGCAGGTTTTGGCCACTGACTGACCTGCCACGAAAGCAACATT-3′ and the reverse primer 5′-CCTGAATGTTGCTTTCGTGGCAGGTCAGTCAGTGGCCAAAACCTGCCACGAGAAAGCAACATTC-3′. Cells stably expressing the miR RNAi vector for CDCP1 and LacZ were established and cultured in medium containing blasticidin (Invivogen) at a concentration of 10 μg/ml for 3 weeks. Two clones expressing the CDCP1 RNAi vector (miCDCP1-1 and -2) were selected by significant suppression of the CDCP1 protein (<10%), and two clones from the control LacZ vector were also selected (miLacZ-1 and -2).

Soft-agar colony assay. Six-well tissue culture plates were coated with a layer of RPMI 1640-10% FBS containing 0.5% ultrapure agarose (Invitrogen). Subconfluent A549 cells transfected with the dicer siRNA or miR RNAi vector-expressed clone were treated with EDTA, washed in phosphate-buffered saline twice, and resuspended in RPMI 1640-10% FBS at 6×10^3 cells/ml. Then, a 500-μl cell sample was added to 1 ml of RPMI 1640-10% FBS containing 0.5% ultrapure agarose (final concentration, 0.33%). The cells were plated on the coated tissue culture plates, allowed to solidify, and then placed in a 37°C incubator. After 30 days, colonies were scanned using a GS-800 calibrated densitometer (Bio-Rad), and the numbers of colonies per well were determined. Soft-agar assays were performed three times.

Immunoprecipitation and Western blotting. Cell lysates were prepared with protease inhibitors in PLC buffer (10 mM Tris-HCl, pH 7.5, 5 mM EGTA, 150 mM NaCl, 1% Triton X-100, 10% glycerol, 10 μg/ml aprotinin, 1 mM sodium orthovanadate [Na_3VO_4], and 100 μg/ml leupeptin). The protein concentration was measured by BCA protein assay (Pierce). For purification, 1 μg of monoclonal or affinity-purified polyclonal antibody was added to the proteins, which were then incubated with 500 μl (2 mg/ml) of cell lysate for 2 h at 4°C. Next, they were precipitated with protein A- or protein G-agarose for 1 h at 4°C. The immunoprecipitates were extensively washed with PLC buffer and prepared for Western blotting.

For Western blotting, samples were separated on sodium dodecyl sulfate-polyacrylamide gel electrophoresis and transferred to a polyvinylidene difluoride membrane (Immobilon-P; Millipore). After blocking of the membrane with blocking buffer (Blocking One; Nakarai Tesque), the membrane was probed with antibodies for detection. The membrane was further probed with HRP-conjugated anti-mouse, anti-rabbit, or anti-goat IgG (1:4,000) to visualize the reacted antibody.

Images were captured by a molecular imager (GS-800; Bio-Rad), and the density of each smear was quantified using Quantity One software (Bio-Rad).

Identification of CDCP1. Isolated GST-FynSH2 protein coupled with cyanogen bromide (CNBr) was used to purify the 135-kDa and 70-kDa proteins from the A549 cells cultured for 48 h on MPC-coated plates in growth medium. Briefly, 3×10^7 suspended A549 cells in a total of 400 dishes (10-cm dish; 30 ml culture medium) were collected and lysed in PLC buffer. The cell lysate was rotated for 8 h at 4°C with GST-FynSH2 protein and washed four times using PLC buffer before being eluted with GST-FynSH2-coupled proteins using 8 M urea buffer (8 M urea, 10 mM Tris-HCl, pH 7.4, 150 mM NaCl, 1% Triton X-100). Secondly, the eluted sample was dialyzed three times against a 100-fold volume of dialysis buffer (10 mM Tris-HCl, pH 7.4, 150 mM NaCl, 1 mM Na_3VO_4), and then the sample was affinity purified with antiphosphotyrosine monoclonal antibody (4G10) coupled with CNBr. 4G10-coupled proteins were washed four times using PLC buffer and once using heptyl-glucoside buffer (10 mM Tris-HCl, pH 7.4, 150 mM NaCl, 0.1% heptyl-glucoside). Next, the samples were eluted using 0.1 M phenylphosphate in heptyl-glucoside buffer. The purified 135-kDa and 70-kDa proteins were concentrated, electrophoresed, and blotted onto a ProBlott membrane (Applied Biosystems). After visualization with colloidal gold total-protein stain (Bio-Rad), the isolated 135-kDa and 70-kDa bands were analyzed by mass spectrometry. Four sets of amino acid sequences determined from the 135-kDa band and an amino acid sequence determined from the 70-kDa band indicated that both the 135-kDa and 70-kDa proteins were CDCP1.

Apoptosis assay. Each cell was treated with EDTA, and 1×10^4 cells were reseeded onto normal or MPC-coated 96-well plates. After 24 h, the cells were lysed and used for the detection of apoptosis. Apoptosis levels were determined using a cell death ELISA kit (Roche Molecular Biochemicals), which detects the presence of nucleosomes in the cytoplasm of apoptotic cells. The absorbance of the samples was measured at a wavelength of 405 nm using a microplate reader model 550 (Bio-Rad).

BrdU incorporation assay. Cell proliferation was analyzed with the cell proliferation ELISA BrdU kit according to the manufacturer's instructions (Roche Molecular Biochemicals) based on the measurement of 5-bromo-2′-deoxyuridine (BrdU) incorporation during DNA synthesis of proliferating cells. Briefly, A549 cells were cultured in triplicate for 24 h in 96-well plates (1.0×10^4 cells/well) with or without cell attachment. The cells were subjected to BrdU incorporation for 6 h. The colorimetric change was measured at 450 nm on a microplate reader model 550 (Bio-Rad).

Infection of retroviral constructs. The retroviral vectors PQCXIN (Clontech) and pCMSCVbsd were used to express human CDCP1 (WT) and Y734F with a FLAG tag at the C terminus and full-length cDNA of Fyn kinase with a double HA tag at the C terminus (FynHA), respectively. pCMSCVbsd contains the blasticidin resistance gene in place of the puromycin resistance gene of pCMSCVpuro (20). These retrovirus vectors were converted into the destination vectors with a vector conversion kit (Invitrogen). The cDNA segments were first cloned into pDONR221 and then into the destination vector, pDEST-PQCXIN or pDEST-CMSCVbsd, according to the manufacturer's instructions (Invitrogen). The production of recombinant retroviruses was performed as described previously (25). Briefly, the retroviral vector and the packaging construct pCL-10A1 were cotransfected into 293T cells using TransIT-293 (Mirus Co., Madison, WI) according to the manufacturer's instructions, and culture fluid was harvested 48 to 72 h posttransfection. H322 cells were infected with the viral fluid in the presence of 4 mg/ml Polybrene, and the infected cells were selected in the presence of 800 μg/ml G418 or 5 μg/ml blasticidin. For combinations of retroviral infections, cells were first transduced with CDCP1 and then with Fyn kinase.

Experimental metastasis assay. Female BALB/cA1c1-nu/nu nude mice were purchased from CLEA Japan Inc. All of the mice used in these experiments were

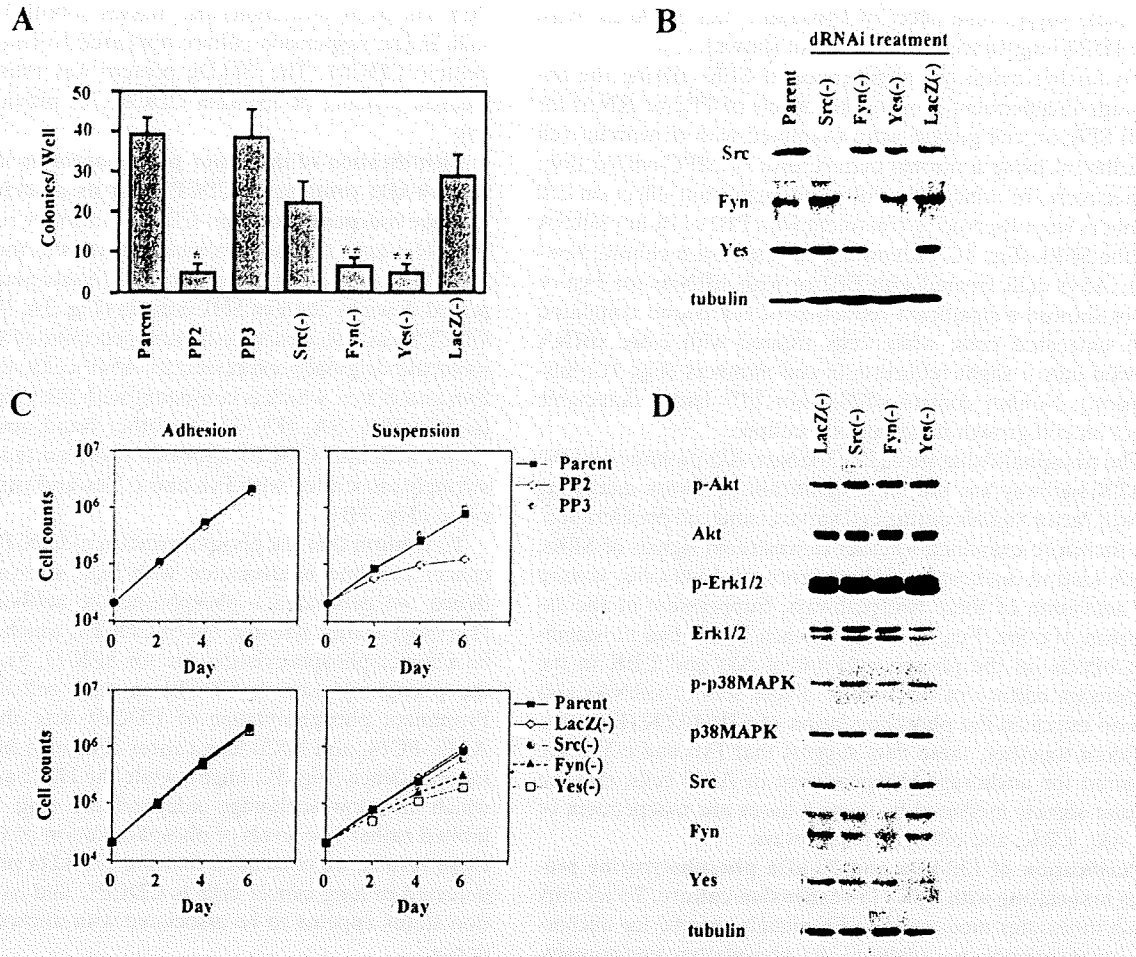

FIG. 1. Anchorage independence of lung adenocarcinoma cells requires SFK. (A) The effect of SFKs on anchorage independence was determined by soft-agar assay. A549 cells were treated with the SFK inhibitor PP2 (10 μM) and SFK dicer RNAi [bars Src(−), Fyn(−), and Yes(−)], and controls [bars Parent, PP3, and LacZ(−)] were seeded onto each soft-agar plate (3×10^3 cells). Colonies equal to and larger than 0.5 mm in diameter were counted after 30 days. The error bars represent standard deviations, and the asterisk indicates statistically significant differences ($P < 0.01$) between the parent and PP2 treatment cells, while the double asterisk indicates statistically significant differences ($P < 0.01$) between LacZ(−) and each of the SFK RNAi treatment cells. (B) A549 cells transiently transfected with c-Src, Fyn, c-Yes, or LacZ dicer RNAi (dRNAi) were incubated for 48 h in culture plates. The cells were lysed and subjected to immunoblotting with the indicated antibodies. (C) Cell growth in A549 cells was subjected to a determination of the number of cells, as described for panel A. Approximately 2×10^4 cells were seeded onto normal (Adhesion) or MPC-coated (Suspension) culture plates with medium. The growth medium was changed every 2 days. The total cell number on each plate was determined every 2 days by a Coulter particle counter z1 (Beckman). (D) SFKs did not affect the phosphorylation of Akt, Erk1/2, or p38MAPK. The lysate of suspended A549 cells transiently transfected with dicer RNAi for each of the SFKs was prepared and subjected to immunoblotting with the indicated antibodies.

6 to 8 weeks old. A549 clones generated by the miR RNAi system and H322 cells were evaluated by experimental metastasis assay, as described by Fidler et al. (8). Briefly, cells (5×10^5 cells/0.2 ml of medium without serum; $n = 6$) were injected into the tail veins of mice. The mice were sacrificed 100 days after cell inoculation for the counting of metastatic nodules. The numbers of lung metastases and nodule formations were determined.

To determine the effect of CDCP1 on tumor growth in nude mice, A549 clones (3×10^6 cells/0.2 ml of medium without serum) were subcutaneously injected into the right flanks of mice. The mice were killed at 30 days. The results are expressed as the mean weight of tumors from three mice ± standard error.

RESULTS

The anchorage independence of lung cancer cells involves SFKs. We first examined the involvement of SFKs in the anchorage independence of A549 lung adenocarcinoma cells using the colony formation assay on soft agar with or without PP2, an SFK inhibitor (Fig. 1A). A549 cells and cells treated with PP3, an inactive derivative of PP2, formed a similar number of colonies in soft agar, while the addition of PP2 caused a significant decrease in the numbers of colonies. A similar effect of PP2 was observed in most lung cancer cells, such as the PC3, PC14, H520, and LK2 cell lines (data not shown).

To determine which member of the SFKs mainly contributes to the anchorage independence of A549 cells, individual expression of c-Src, Fyn, and c-Yes was downregulated using RNAi technology (Fig. 1B), and colony formation assays were performed on soft agar (Fig. 1A). A549 cells treated with Fyn or c-Yes siRNAs formed significantly fewer colonies than the control cells treated with LacZ siRNA, while cells treated with c-Src siRNA formed slightly fewer colonies. We also observed

a similar suppressive effect of Fyn and c-Yes RNAi in PC14 and H520 lung cancer cells (data not shown).

To further assess the significance of SFKs during the anchorage-independent growth, the effects of PP2 or RNAi for each SFK on cell growth were examined with or without cell attachment using a normal culture dish or MPC-coated dish, respectively. In adherent culture, no significant effect on cell numbers was observed by treatment with PP2 or by any siRNA for the SFKs (Fig. 1C, Adhesion). In suspension culture, however, A549 cells treated with PP2 or with siRNAs for Fyn or c-Yes showed a significant reduction of cell counts compared with untreated cells, while cells treated with c-Src siRNA showed only a slight reduction in cell numbers (Fig. 1C, Suspension). Neither control siRNA nor PP3 had a detectable effect on cell growth in suspension culture.

The phosphatidylinositol (PI) 3-kinase Akt pathway and the MAPK pathway are the most significant pathways mediating growth factor signals during cell survival and cell proliferation. We therefore examined whether downstream signals of SFKs, which lead to anchorage independence of A549 cells, involve the activation of these two pathways. Suppression of the expression of c-Src, Fyn, or c-Yes by each RNAi had no significant effects on the phosphorylation of Akt and ERK in the suspension culture of A549 cells. These sets of siRNAs also had no effect on the phosphorylation of p38MAPK (Fig. 1D).

Taken together, these data suggest that Fyn and c-Yes are required for anchorage independence in A549 cells, and the cellular signals mediated by these kinases are independent of the Akt, ERK, and p38MAPK pathways.

Purification of 135-kDa and 70-kDa phosphotyrosine proteins associating with SFKs in suspension culture. To identify which molecules mediate the SFK signals specific for anchorage independence, we analyzed the phosphotyrosine-containing proteins that bind to SFKs. Among the proteins associated with SFKs, two proteins with molecular masses of 135 kDa and 70 kDa were prominently phosphorylated, even in suspension culture (Fig. 2A), and these proteins were also phosphorylated in PC14 and H520 cell lines, which also exhibit a high level of anchorage independence (Fig. 2A, High). In contrast, the H322 and H157 cell lines, which formed a small number of colonies in soft agar (Fig. 2A, Low), displayed rather lower levels of phosphorylation of these two proteins (Fig. 2A). Using these results, we sought to identify proteins that function as downstream mediators of SFKs in anchorage-independent growth.

As several antibodies against the known phosphoproteins failed to recognize the 135-kDa and 70-kDa proteins, we applied affinity purification. Using A549 cells cultured for 48 h with and without cell attachment, these 135-kDa and 70-kDa proteins were pulled down with the Fyn SH2 domain more efficiently under suspension conditions (Fig. 2B). A total of $\sim 1.2 \times 10^{10}$ cells in suspension culture were first purified with the Fyn SH2 domain. After purification by a second affinity column using a 4G10 antiphosphotyrosine antibody, samples were analyzed by Western blotting (Fig. 2C, WB) and colloidal gold total-protein stain (Fig. 2C, G). Bands corresponding to the two proteins were cut out and analyzed by mass spectrometry. Four peptides from the 135-kDa band and one peptide from the 70-kDa band were determined by mass spectrometry to be the recently identified membrane protein CDCP1 (Fig. 2C). The proteins at molecular masses of both 135 kDa and 70 kDa in the suspension culture appeared to contain the single protein CDCP1. The 70-kDa protein was estimated to be a cleaved product of 135-kDa CDCP1, as previously reported (5).

Identification of the major phosphoprotein of the 135-kDa and 70-kDa proteins as CDCP1 and its association with anchorage independence. Anti-CDCP1 antibody recognized proteins of exactly the same molecular masses as the 135-kDa and 70-kDa proteins both in the whole-cell lysate and in the sample pulled down by the Fyn SH2 domain (Fig. 3A, WCL and PD). CDCP1 was also clearly coimmunoprecipitated with each SFK molecule originally expressed in A549 cells, especially with Fyn and c-Yes, which is consistent with the original 135-kDa protein (Fig. 3A, IP). On the other hand, immunoprecipitation with anti-CDCP1 antibody revealed that CDCP1 was strongly associated with Fyn and c-Yes and very weakly with c-Src (Fig. 3B).

To confirm that the phosphorylation of CDCP1 in each lung cancer cell line is associated with high anchorage independence, we generated a phosphospecific antibody (p-CDCP1 [Tyr734]) against tyrosine 734 of CDCP1, which is reported to be a major phosphorylation site for SFK (1, 5), and analyzed the phosphorylation of CDCP1 in each cell line (Fig. 3C). Prominent phosphorylation of CDCP1 was observed in the A549, PC14, and H520 lung cancer cells with high anchorage independence (Fig. 3C, High), while the H322 and H157 cells, which have low anchorage independence (Fig. 3C, Low), exhibited rather low levels of phosphorylation of CDCP1. From these results, we concluded that the 135-kDa phosphoprotein detected in lung cancer cells is CDCP1, and its phosphorylation status appears to be associated with anchorage independence.

We examined whether the phosphorylation of CDCP1 is altered with or without cell attachment in the culture. After detachment of A549 cells with EDTA, the cells were either plated on a normal dish to cause readhesion or plated on an MPC-coated dish to grow in suspension for 48 h. Under either plating condition, the phosphorylation level of CDCP1 was continuously increased until 24 h; however, it exhibited a sudden decrease at 48 h in adhesion culture, while it increased further in suspension culture (Fig. 3D). Notably, these dynamic changes of phosphorylation during cell suspension and readhesion appear to partially reflect the change in the expression level of CDCP1.

CDCP1 is a regulator of anoikis resistance in lung adenocarcinoma. Next, we checked whether CDCP1 is involved in the regulation of the anchorage independence of A549 cells under the control of SFK activity. For this purpose, we obtained the stable A549 cell clones miCDCP1-1 and miCDCP1-2, which showed suppressed expression of the CDCP1 protein, by using the siRNA for CDCP1 with a BLOCK-iT Pol II miR RNAi expression vector system (Fig. 4A). Both of the clones formed significantly fewer colonies in the soft-agar assay than the LacZ clones (Fig. 4B), suggesting that CDCP1 is actually required for the anchorage independence of A549 lung adenocarcinoma.

Anchorage independence may reflect the persistence of growth and/or survival of cancer cells in suspension; therefore, the effects of CDCP1 expression in suspended cells on cell

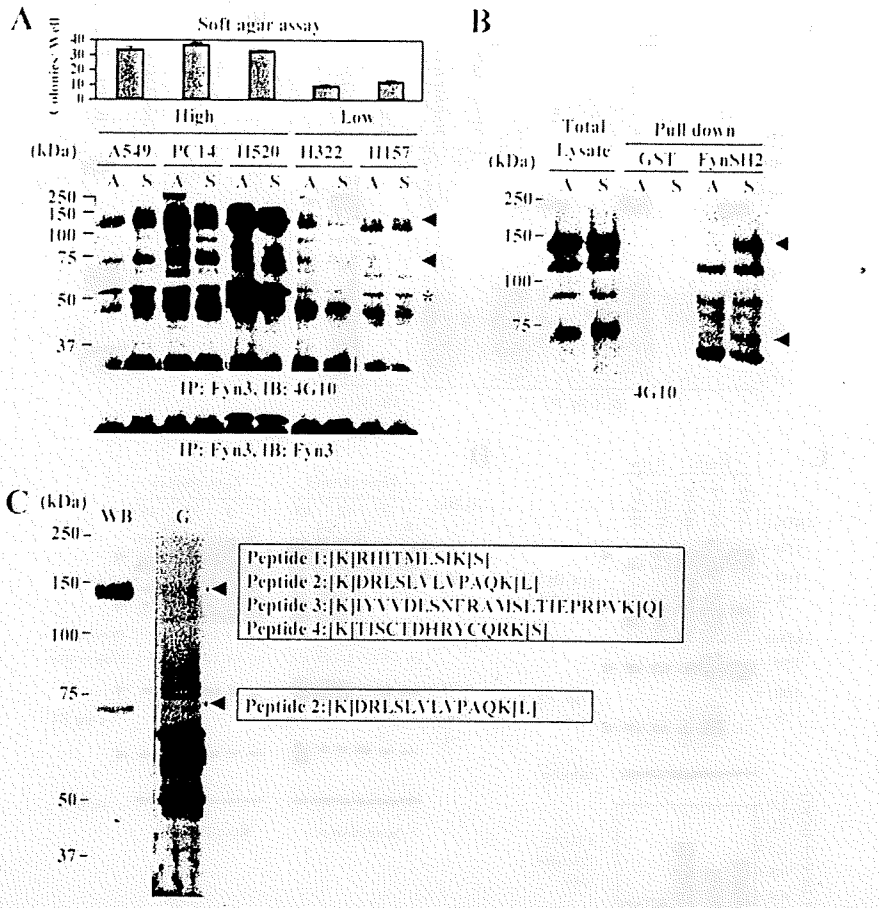

FIG. 2. Purification of phosphotyrosine-containing 135-kDa and 70-kDa protein-forming complexes with SFKs in suspension culture. (A) Anchorage independence in a series of lung cancer cell lines was examined by soft-agar assay (top). The large number of colonies formed in the lung cancer cell lines A549, PC14, and H520 (High) and the small number of colonies formed in the H322 and H157 cell lines (Low) cultured for 48 h under both adhesion and suspension conditions were collected and subjected to immunoprecipitation (IP) with anti-Fyn (Fyn3) antibody and immunoblotting (IB) with antiphosphotyrosine (4G10) antibody. Phosphotyrosine-containing proteins coimmunoprecipitated with Fyn at the molecular masses of 135 kDa and 70 kDa are indicated by arrowheads. The asterisk indicates phosphorylated Fyn. The expression of Fyn in each cell lysate was confirmed by immunoblotting (bottom). A, adhesion; S, suspension. The error bars represent standard deviations. (B) GST-FynSH2 protein generated by *Escherichia coli* was used to pull down the lysate of A549 cells cultured under adhesion or suspension conditions. The isolated samples were immunoblotted with antiphosphotyrosine (4G10) antibody. The arrowheads indicate the phosphotyrosine-containing 135-kDa and 70-kDa proteins. (C) Phosphotyrosine-containing proteins (135 kDa and 70 kDa) were purified according to the protocol described in Materials and Methods. Aliquots of the purified 135-kDa and 70-kDa phosphotyrosine-containing proteins were examined by Western blotting (WB) using antiphosphotyrosine (4G10) antibody, and the remaining samples were stained with colloidal gold total-protein stain (G). Four peptides determined by mass spectrometry (peptides 1 to 4) were identified within the sequence of CDCP1.

proliferation and on cell apoptosis were individually examined. Each miCDCP1 clone in suspension culture showed an increased level of apoptosis compared with miLacZ clones (Fig. 4C). In contrast, no significant change in the cell growth level was observed in each of the miCDCP1 and miLacZ clones compared with the parental A549 cells in suspension culture (Fig. 4D). Importantly, there was no significant change in either cell growth or apoptosis in the adhesion culture (Fig. 4C and D).

We also examined the effect of the expression of phosphorylated CDCP1 on cell proliferation and cell apoptosis using H322 lung adenocarcinoma cells with low anchorage independence. CDCP1 (WT) and/or Fyn kinase with double HA tags at the C terminus (FynHA) were expressed in H322 cells by retroviral vectors, and the expression was checked by Western blotting (Fig. 5A). Additionally, a CDCP1 mutant lacking a putative SFK-binding site (Y734F) was also expressed (2). An increased level of phosphorylation of CDCP1 was observed in H322 cells overexpressing both WT and Fyn kinase (Fig. 5A, WT+FynHA), which caused an inhibition of apoptosis in suspension culture (Fig. 5B). These changes were not observed with either Fyn kinase or WT CDCP1 alone. On the other hand, expression of Y734F alone increased the level of apoptosis in suspension culture, suggesting a dominant-negative effect of this CDCP1 mutant (Fig. 5B, Y734F). A slight enhancement of cell proliferation in suspension culture was observed by expressing Fyn kinase and either WT or mutant CDCP1, but this change was not significant (Fig. 5C).

These results suggest that phosphorylation of CDCP1 confers anchorage independence through the inhibition of apoptosis. In other words, phosphorylation of CDCP1 regulates resistance to anoikis in lung cancer cells.

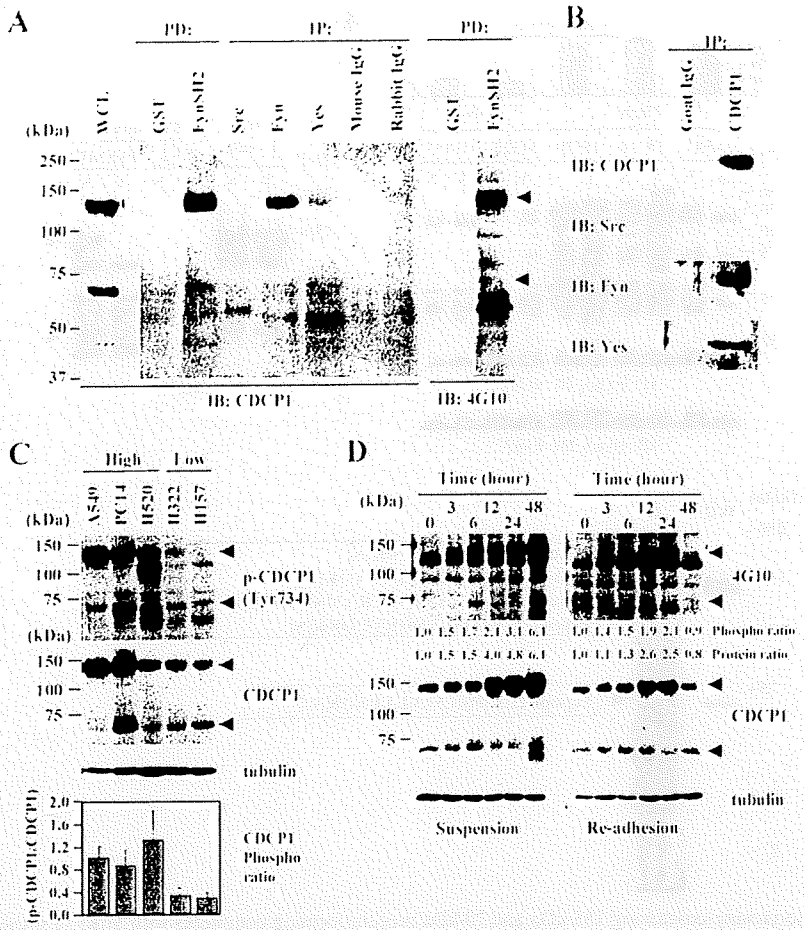

FIG. 3. Identification of the 135-kDa and 70-kDa proteins as CDCP1 and its phosphorylation associated with anchorage independence. (A) The lysate of A549 cells was subjected to whole-cell lysate (WCL) or pull-down assay with GST-FynSH2 protein (PD) or immunoprecipitated with anti-c-Src, anti-Fyn, and anti-c-Yes antibodies (IP) and immunoblotted (IB) with anti-CDCP1 antibody. The same blot was rehybridized with antiphosphotyrosine (4G10) antibody. (B) The lysate of A549 cells was immunoprecipitated with anti-CDCP1 antibody (ab1377) or goat IgG as indicated. The precipitates were subjected to immunoblotting with anti-c-Src, anti-Fyn, anti-c-Yes, and anti-CDCP1 antibodies. (C) The large number of colonies formed by the lung cancer cell lines A549, PC14, and H520 (High) and the small number of colonies formed by the H322 and H157 cell lines (Low) cultured for 48 h in the suspension condition were collected and subjected to immunoblotting with anti-phospho-CDCP1 (Tyr734) and CDCP1 antibodies. This experiment was performed three times. The ratio of the phosphorylation level in each lung adenocarcinoma cell was measured as described in Materials and Methods. The error bars represent standard deviations. (D) Time course analysis of CDCP1 expression and phosphorylation with or without cell attachment. A549 cells were reseeded on normal cell culture plates and an MPC-coated plate at a density of 1.5×10^5 cells per plate with complete medium. For the preparation of the reseeding cells, 2 mM EDTA/Hanks' balanced salt solution was used to detach the cells. For each time point, cells were collected and subjected to immunoblotting with the indicated antibody. The same membrane rehybridized with antitubulin antibody confirmed the concentration of total proteins in each lysate (tubulin). The arrowheads indicate CDCP1.

PKCδ is a signal molecule downstream of CDCP1 during anoikis resistance in lung adenocarcinoma. CDCP1 protein has been shown to bind PKCδ in a phosphorylation-dependent manner (2). PKCδ is a regulator of apoptosis, and it has been reported that the phosphorylation of PKCδ requires the activity of SFKs (37). By treatment with the SFK inhibitor PP2, both the association of PKCδ with CDCP1 and the phosphorylation of PKCδ at Tyr311 were clearly inhibited (Fig. 6A). CDCP1 (WT) and the CDCP1 protein with a point mutation at Tyr734 (Y734F) were C-terminally FLAG tagged and expressed in COS7 cells. After transfection with each plasmid, the association of the Fyn SH2 domain with WT and Y734F mutants was examined. The Fyn SH2 domain was able to pull down the WT but not the Y734F mutants (Fig. 6B, PD: Fyn SH2). The levels of tyrosine phosphorylation of Y734F mutants was much lower than that of the WT in A549 cells (Fig. 6B, IB: 4G10), suggesting that Tyr734 of CDCP1 directly binds to Fyn and that the association is essential for the phosphorylation of CDCP1. The association between CDCP1 and PKCδ was also impaired in the Y734F mutant compared with the WT, indicating that the phosphorylation of CDCP1 is required for the association.

Overexpression of Y734F in A549 cells also blocked the association between PKCδ and CDCP1 and the phosphorylation of PKCδ at Tyr311 (Fig. 6B). Moreover, treatment with CDCP1 siRNA also decreased the phosphorylation level of PKCδ (Fig. 6C). In addition, the phosphorylation level of PKCδ at Tyr311 was elevated in H322 cells by overexpressing both WT CDCP1 and Fyn kinase but not significantly with either the WT, the Y734F mutant, or Fyn kinase alone (see the